Journal Pre-proofs

Research papers

# Impact of Climate Change and water use policies on hydropower potential in the south-eastern Alpine region

Bruno Majone, Francesca Villa, Roberto Deidda, Alberto Bellin

DOI: https://doi.org/10.1016/j.scitotenv.2015.05.009

Reference: STOTEN 17747

To appear in: Science of the Total Environment

Received date: 10 January 2015

Revised date: 17 April 2015

Accepted: 3 May 2015

Available online: 13 May 2015

Version recorded: 10 December 2015

**Please cite this article as**: Majone, M., F. Villa, R. Deidda, A. Bellin, Impact of Climate Change and water use policies on hydropower potential in the south-eastern Alpine region. *Science of the Total Environment,* Volume 543, Part B, 965-980, (2016), doi: https://doi.org/10.1016/j.scitotenv.2015.05.009

# Impact of Climate Change and water use policies on hydropower potential in the south-eastern Alpine region

Bruno Majone[a,*], Francesca Villa[a], Roberto Deidda[b,c], Alberto Bellin[a]

[a]Department of Civil, Environmental and Mechanical Engineering, University of Trento, Via Mesiano 77, I-38123 Trento, Italy
[b]Department of Civil and Environmental Engineering and Architecture, University of Cagliari, Via Marengo 2, I-09123 Cagliari, Italy
[c]CINFAI, Consorzio Interuniversitario Nazionale per la Fisica delle Atmosfere e delle Idrosfere, Piazza N. Maurizi 17, I-62029 Camerino, Italy

**Abstract**

Climate change is expected to cause alterations of streamflow regimes in the Alpine region, with possible relevant consequences for several socio-economic sectors including hydropower production. The impact of climate change on water resources and hydropower production is evaluated with reference to the Noce catchment, which is located in the Southeastern Alps, Italy. Projected changes of precipitation and temperature, derived from an ensemble of 4 Climate Models (CMs) runs for the period 2040-2070 under the SRES A1B emission scenario, have been downscaled and bias corrected before using them as climatic forcing in a hydrological model. Projections indicate an increase of the mean temperature of the catchment in the range $2-4\,K$, depending on the climate model used. Projections of precipitation indicate an increase of annual precipitation in the range between 2% and 6% with larger changes in winter and autumn. Hydrological simulations show an increase of water yield during the period 2040-2070 with respect to 1970-2000. Furthermore, a transition from glacio-nival to nival regime is projected for the catchment. Hydrological regime is expected to change as a consequence of less winter precipitation falling as snow and anticipated melting in spring, with the runoff peak decreasing in intensity and anticipating from July to June. Changes in water availability reflect in the Technical Hydropower Potential (THP) of the catchment, with larger changes projected for the hydropower plants located at the highest altitudes. Finally, the impacts on THP of water use policies such as the introduction of prescriptions for Minimum Ecological Flow (MEF) have been analyzed. Simulations indicate that in the lower part of the catchment reduction of the hydropower production due to MEF releases from the storage reservoirs counterbalances the benefits associated to the projected increases of inflows as foreseen by simulations driven only by climate change.

*Keywords:* Climate change impacts, Alpine region, Water use policies, Water discharge alterations, Hydropower potential

*Highlights*
- First assessment of climate change impact on hydropower in Southeastern Alps, Italy.
- Significant differences in the impacts between hydropower plants within the same catchment.
- Relevant effect of minimum ecological flow regulation on hydropower potential.

*Corresponding author. Tel.: +39 0461 282637; fax +39 0461 282672.
*Email address:* bruno.majone@unitn.it (Bruno Majone)

## 1. Introduction

European Alps are hydrologically relevant since they represent a reliable source of freshwater supply to lowland regions (Viviroli and Weingartner, 2004). Furthermore, the Alpine region has been recognized as a particularly sensitive environment where climate change is expected to influence the river regime with consequent effects on the services offered by the freshwater ecosystem as well as on water resources availability for users in several socio-economic sectors (Viviroli et al., 2011; Beniston, 2012a,b). Current and expected future global warming will cause alterations on streamflow regimes and freshwater ecosystems (Kundzewicz et al., 2014), but impacts on anthropogenic activities such as agriculture, tourism (Rixen et al., 2011) and hydropower are also expected (see e.g., Gaudard et al., 2014).

Given the far reaching services of water resources of the European Alps in sectors ranging from energy production to agriculture and tourism, the need of catchment-scale studies addressing implications of climate change on water availability and flow regime is urgent (Beniston et al., 2011). Several recent studies highlighted that warming will lead in the next decades to changes in the seasonality of river flows as a consequence of less winter precipitation falling as snow and the melting of winter snow occurring earlier in spring (see e.g., Laghari et al., 2012; Finger et al., 2012). Furthermore, a moderate decrease of snow and ice storage is in general projected for 2020 - 2050 with more drastic changes simulated for the second half of the century (see e.g., Lambrecht and Mayer, 2009; Farinotti et al., 2012). High altitute first order streams, with glaciers in their catchment, are expected to experience an increase in winter streamflow, accompanied by a reduction in summer streamflow when the transitional increase in glacier melting will initially compensate for runoff losses due to the reduction of snow melt and precipitation (Bavay et al., 2013).

While almost all climate models (CMs) provide a clear indication of a warmer climate in the future, climate projections of precipitation are much more uncertain due to difficulties of CMs to correctly represent physical processes and local features in the complex orography of the greater Alpine region (GAR). Analyses on instrumental time series from 1800 to 2000 (Brunetti et al., 2006, 2009; Brugnara et al., 2012) give evidence of i) opposite trends in different subregions of the GAR (with significative positive trends in the northern parts and less significative negative trends in the southern parts) and ii) alternations of opposite trends depending on the starting time and the time window length selected for the trend analysis. Contradicting trends of future annual precipitation in the GAR emerge also when comparing different CMs projections, as well as alternations of periods characterized by opposite trends are often present within the temporal evolution of some CM runs (e.g., Gobiet et al., 2014; Finger et al., 2012; Cane et al., 2013).

However, despite the uncertainty related to the identification of possible trend of annual precipitation, most CMs agree in predicting a tendency of higher precipitation in winter/spring and lower precipitation in summer/autumn (Beniston, 2012a; Cane et al., 2013; Finger et al., 2012; Gobiet et al., 2014), in agreement with the trends detected in instrumental time series (Brunetti et al., 2006, 2009; Brugnara et al., 2012). Another problematic issue is related to the seasonal distribution of precipitation: indeed, unimodal (with peak in summer) and bimodal (with peaks in autumn and spring) distributions coexist in the GAR depending on the location and altitude of the investigated station (Brunetti et al., 2006, 2009; Beniston, 2006). Such local features as well as the complexity related to the GAR orography cannot be properly represented by CMs due to their coarse scale resolution and thus require ad hoc error corrections before CM output can be used as forcing of hydrological models (e.g., Finger et al., 2012).

Besides these peculiar features of the GAR area, it is also important to mention that climate change impact assessments on hydrological systems should in principle include an end-to-end consideration of the ”uncertainty cascade” (Wilby and Dessai, 2010). In particular, there has been increasing attention to quantify and reduce the many sources of uncertainty related to emissions scenarios, climate model selection and initial conditions, downscaling techniques including dynamical or statistical methods, hydrological model structures and parameterizations, land use changes and measurements error (see e.g., Caldeira et al., 2003; Funtowicz and Ravetz, 1990; Hawkins and Sutton, 2009; Heikkinen et al., 2006; Morgan and Mellon, 2011; Murphy et al., 2004; Tebaldi et al., 2005; Wilby and Harris, 2006). However, due to the intensive computational effort required, only few studies explicitly compared uncertainty in streamflow predictions arising from all the different source of uncertainty (see e.g., Kay et al., 2009; Chen et al., 2011), concluding that uncertainty derived from global climate modelling is in general greater than that arising from hydrological modeling.

As a consequence of relatively high precipitations and large reliefs, hydropower production largely exceeds the demand of electric energy by the Alpine region. For example, in 2012 hydropower energy accounted for around 13.5% of the national energy production in Italy (GSE, 2013) and was mainly produced by hydropower plants in the Alps, while in Austria and Switzerland hydropower energy satisfies more than 50% of the national request (Zimmermann, 2001). Climate change impacts on hydropower production in the Alpine region may differ depending on both location and typology of hydropower system. Run-of-the-river power plants are directly influenced by the change in the water discharge regime, whilst hydropower plants with significant storage volume are more flexible and may adopt different management strategies to compensate for modifications, depending also from the evolution of the energy market (Beniston and Stoffel, 2014).

The projection of hydropower productivity of existing power plants is thus a relevant issue worldwide. Kumar et al. (2011) estimated that by 2070, hydropower potential for the whole Europe will reduce of about 6%. However, this estimate is the result of a larger reduction in the Mediterranean area, partially compensated by an increase in the northern and eastern Europe. Markoff and Cullen (2008) found that climate change has the potential to seriously impact the hydropower system of the Columbia river basin (USA) with uncertainty in projections of precipitation change appearing more important with respect to that arising in projections of temperature change. Minville et al. (2009) evaluated the impacts and adaptation to climate change of the water resource management system of the Peribonka River (Canada), which is intensively exploited for hydropower production. By adopting the output of a single Regional climate model, they found that annual mean hydropower production would decrease for the period 2010-2039 and then increase by 9.3% and 18.3% during the periods 2040-2069 and 2070-2099, respectively. Vicuna et al. (2008) investigated the impacts of climate change on hydropower generation in the Sierra Nevada chain (USA) by considering climatic outputs from two GCMs under two emissions scenarios. In particular, they found that hydroelectric systems, located in basins with significant inflows during the late spring and early summer months, will be significantly affected by projected changes in the timing of streamflows as a consequence of insufficient storage capacity. Vicuna et al. (2010) and Raje and Mujumdar (2010) assessed the effects of climate change on multipurpose reservoirs in the Merced (USA) and Mahanadi (India) river basins, respectively, by considering an adaptive management strategy mimicking a real operational context using climate change scenarios from eleven and three GCMs, respectively. Koch et al. (2011) projected the hydropower production of the Upper Danube basin to the period 2051 - 2060 by means of a physically-based hydrological model, coupled with a simple hydropower module, and considering 16 climate change scenarios resulting from a stochastic downscaling applied to the outputs of two different regional climate model, under SRES-A1B emission scenario. The main conclusions of this work is that in the period 2051 - 2060 a moderate to severe reduction is expected, depending on the adopted climate model. Schaefli et al. (2007) analyzed the water resource system connected to the Mauvoisin reservoir (Swiss Alps) focusing on the quantification of uncertainty arising from both climate scenarios and hydrological modeling; results obtained indicate a significant reduction of water resources availability due to the effect of climate change. Hänggi and Weingartner (2012) analyzed the variations of water volumes available for hydropower production at several high-altitude locations in the Swiss Alps during the last century and observed a general increasing trend in the annual water volume. The simulations conducted by Finger et al. (2012), including uncertainty in the climate scenarios, projected a moderate decrease of incoming streamflow to the Mattmarksee lake (Swiss) in the period 2037 - 2064, followed by a major decrease by the end of the century, with the consequent need to change hydropower production schemes to overfill Mattmarksee lake. Recently, a few studies pointed out the importance of considering both hydrological processes and electricity market behavior in order to perform reliable climate change impact assessments on hydropower production (Gaudard et al., 2013, 2014; Maran et al., 2014). Although the results of these studies, conducted in the Swiss and Northwestern Italian Alps, are to some extent dependent on the position of the hydropower system, they concur in concluding that a new adaptive management of hydropower plants may mitigate projected losses due to modified climatic conditions. All the above studies evidenced a significant dependence of the projected hydropower production on the type of hydropower system and its location, thereby calling for plant-specific analyses to evaluate the effect of climate change on hydropower production.

However, to our best knowledge none of the previous studies investigated the concurrent impact of climate change and water uses, such as the introduction of a minimum ecological flow regulation and other constraints due to concurrent uses, on hydropower potential. Only the work of François et al. (2014) partially addressed this issue by analyzing the sensitivity of marginal storage water value (defined as the marginal value of the future benefits obtained from an additional unit of storage water volume) to projected changes in regional climatology, as well as in the water demand for hydropower production and/or maintenance of a minimum reservoir level during summer periods. The study, conducted with reference to a single reservoir system located in French Alps, evidenced that the equilibrium between water resources availability and demand is strictly correlated with the considered future scenario, being in particular more sensitive to warmer conditions than to drier ones.

As a further constraining element, it should be considered that reservoir levels in the Alps are typically constrained by touristic and landscaping requirements, and in some case by the need to guarantee certain storage volumes for agricultural uses during well defined irrigation periods. This is a relevant issue since projected modifications in the hydrological cycle can likely lead to possible conflicts among different and often competing water uses and may require the change of the protocols regulating concurrent uses. In this context the Noce river basin, which is located in South-Eastern Italian Alps, is an interesting study area with several concurrent uses by hydropower, touristic activities (canoeing, rafting and sport fishing) and agriculture. The allocation of water resources among the different uses is complicated by the fact that not all the uses are necessarily in conflict (La Jeunesse et al., 2015, this issue). Hydropeaking (i.e., artificial streamflow fluctuation in rivers as a consequence of hydropower plants releases) due to discontinuous hydropower production, which is the direct consequence of the daily variations of the energy price, for example, has a negative impact on the freshwater ecosystem, but it is considered positive for activities such as canoeing and rafting, which may take advantage from the increase of the streamwater level at daylight. In this catchment water allocation and transfers are performed according to the protocols included in the Water Uses General Act (PGUAP, 2006) of the Province of Trento (available online at http://pguap.provincia.tn.it), which defines for each water use the Minimum Ecological Flow (MEF) releases in order to satisfy water demand of downstream territories and to maintain the ecological functionality of the river as required by the European Water Framework Directive (WFD, European Commission, 2000).

This study addresses questions that are relevant also at a regional scale, because of the lack of studies investigating the potential impacts of climate change on hydrological cycle and hydropower production in the south-eastern Alpine region and specifically in the Trentino - Alto Adige region (Italy). This is relevant since total installed capacity in the 588 hydropower plants located in Trentino - Alto Adige is of 3205 MW (GSE, 2013), with an energy production in 2012 of 9097 GWh, which corresponded to 21.7% of the whole Italian hydropower production. In particular, plants located within the Noce river basin contribute substantially with a total installed capacity of 317 MW, which accounts for 10% of Trentino - Alto Adige total capacity. The projected impacts of climate change on hydropower potential are thus examined by coupling outputs from an ensemble of 4 CM experiments with a distributed hydrological model. Despite the analysis of the different sources of uncertainty in the modelling chain is limited only to that arising from climate model selections, this study provides a robust estimate of changes in water resources and hydropower potential due to the projected climate changes in the region. The comparative assessment of the effects of climate change and water use policies on hydropower potential represents also a novelty of the present work.

The paper is organized as follows: Section 2 presents a description of the study area; Section 3 describes the hydrological model and parameters identification; climate change projections are introduced in Section 4; validation of the hydrological model is discussed in Section 5; the main results on the possible effects of climate change on the hydrological system and hydropower potential of the catchment are presented in Sections 6 and 7, while conclusions are drawn in Section 8.

## 2. Study site

The study site is the Noce catchment, located in the Dolomites region, Northwestern Italy. It rises from the reliefs of the Ortles-Cevedale and Adamello Presanella groups and flows first to East, but in its middle course it turns to South-East and enters the river Adige close to the municipality of Mezzolombardo a few kilometers North of the city of Trento. Its main course is $82\,km$ long and the total contributing area is of $1,367\,km^2$ (see Fig. 1).

Headwater streams receive the contribution from the glaciers of the Ortles-Cevedale and Adamello-Presanella groups. In the middle course the river receives several tributaries (i.e. Vermigliana, Meledrio and Tresenica creeks on the right bank and Rabbies and Novella creeks in the left bank). The dominance of the contribution from the Presena and Presanella glaciers in the streamflow timing and biophysical characteristics of the Vermigliana creek, one of the most important headwater creeks of the catchment, has been evidenced in a characterization study by Chiogna et al. (2014), which the reader is referred to for further details.

Land use is chiefly timber forests (56.5%), bare rocks (16.4%), pastures (15.4%) and agricultural fields (6.2%). Urban areas occupy 2.8% of the territory, with the remaining surface occupied by water bodies and glaciers. Paragneis dominates the geology of the northern part of the catchment, ortogneiss, micaschists and phyllite are mostly present in the center and tonalite can be found in the Eastern and Southern parts where karst phenomena have been also observed. Climate is cold and wet with a mean annual temperature of 3.9°$C$ and mean annual precipitation of 1172 mm/year (averages refer to the period 1970-2000), with significant snowfalls in winter.

Five major hydropower plants with a total installed capacity of 278.3 MW are located along the river: Malga Mare, Cogolo1, Cogolo2, Taio and Mezzocorona (see Fig. 1). Main characteristics of each hydropower plant are reported in Table 1. Hydropower production of these power plants is regulated by 5 reservoirs with a total storage capacity of $203 \cdot 10^6 m^3$ (Table 1): Careser, Pian Palù, Malga Mare, Santa Giustina and Mollaro. These reservoirs are managed by licensed hydropower companies according to the rules dictated by specific protocols included in the Water Uses General Act (PGUAP, 2006) of the Province of Trento (available online at http://pguap.provincia.tn.it). The protocols define in detail the $MEF$ releases that should be guaranteed to satisfy the water demand of downstream territories and to maintain ecological functionality of the river (see Table 2). Two small powerhouses are located at the toe of Santa Giustina and Mollaro reservoirs in order to exploit $MEF$ releases. Furthermore, flood risk is managed by allocating extra storage capacity to the reservoirs.

Besides the presence of large hydroelectric power plants the basin is intensively exploited with a large number of small withdrawals associated to a variety of water uses: small run-of-the-river power plants (i.e. average nominal capacity < 3 MW) and agricultural, civil and industrial withdrawals (see, Bellin et al., 2015, for further details). Total average nominal capacity of small run-of-the-river power plants is 21 MW, which accounts for around 16% of total average nominal capacity of the catchment (134.9 MW). $MEF$ constraints as foreseen by PGUAP (2006) are also imposed at each licensed withdrawal location. Since hydropower production in the Noce catchment is mainly associated to storage reservoirs, in the ensuing sections the analysis will concentrate only on the systems with average nominal capacity larger than 3 MW.

Table 1: Main characteristics of the reservoirs present within the Noce river basin.

| | **Hydropower Plant** | **Max. Storage** $[10^6 m^3]$ | **Storage capacity** $[10^6 m^3]$ | **Max. Water Flow** $[m^3/s]$ | **Installed capacity** $[MW]$ | **Average nominal capacity** $[MW]$ | **Static head** [a] $[m]$ |
|---|---|---|---|---|---|---|---|
| *Pian Palù* | Cogolo2 | 15.510 | 15.266 | 7.6 | 47.8 | 10.8 | 576.5 |
| *Careser* | Malga Mare | 15.580 | 15.247 | 3 | 12.5 | 3.4 | 609.6 |
| *Malga Mare* | Cogolo1 | 0.033 | 0.033 | 6.4 | 49.4 | 16.3 | 756.4 |
| *S. Giustina* | Taio | 186.294 | 171.670 | 66 | 105.0 | 40.8 | 139.9 |
| | S. Giustina MEF | - | - | 2.1 [b] | 2.2 | 2.1 | 100.0 |
| *Mollaro* | Mezzocorona | 0.864 | 0.864 | 60.0 | 63.6 | 39.8 | 121.7 |
| | Mollaro MEF | - | - | 2.44 [b] | 0.7 | 0.7 | 26.0 |

[a] Static head is defined as the difference between the average water level in the reservoir and the level of the turbine nozzle.
[b] These values refers to the maximum water flows allowed by water authority during the period 2000-2006. For simulations of future periods it is assumed that these flows will be equal to the maximum of monthly MEF releases that are prescribed for the catchment after 2017 (see Table 2).

## 3. Hydrological Model

In the present work, the semi-distributed modeling system GEOTRANSF (Bellin et al., 2015) has been adopted for simulating hydrological cycle at the catchment scale. Recently, GEOTRANSF has been used to conduct climate change impact studies on streamflow and water resources in the Gàllego catchment, Spain (Majone et al., 2012; Graveline et al., 2014). Furthermore, it has been applied in a number of studies to assess the local impact of the water uses in the Province of Trento, which includes the Noce catchment.

GEOTRANSF is designed to work with minimal meteorological information consisting in precipitation and temperature data. However, observed streamflow data are needed when applying inverse modeling to infer model parameters from observational data. River network topology is extracted from a Digital Elevation Model (DEM), while maps of soil type and land use are used to assign spatially variable parameters to the infiltration model.

The modeling system is modular and includes modules for snow accumulation and melting, infiltration, evapotranspiration, sub-surface flow, deep percolation and baseflow. Model structure is presented in Fig. 2 along with the corresponding parameters. A short description of the parameters and their meaning is provided in Table 3. GEOTRANSF is built around two geomorphological units which are combined in such a way to obtain a distributed

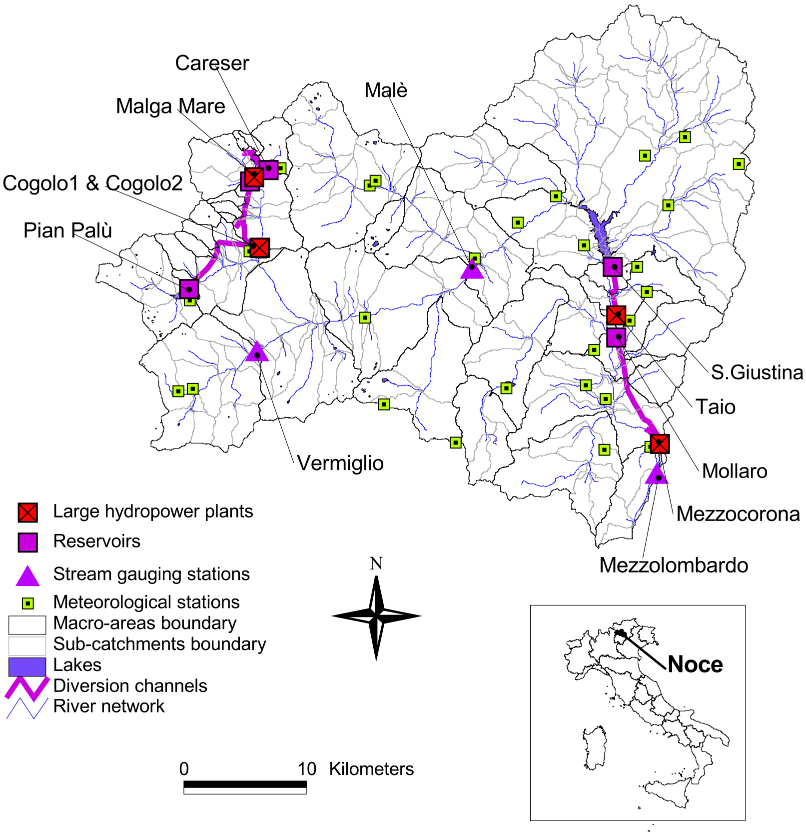


Figure 1: Map of the Noce river basin showing the subdivision in macro-areas and sub-catchments, the locations of water discharge gauging stations, reservoirs, meteorological stations, artificial channel network and large hydropower plants (i.e. average nominal power production capacity > 3 MW). Malga Mare hydropower plant is connected with the Careser reservoir and the water elaborated is then discharged into the homonymous reservoir. Cogolo 1 plant collects the water from Malga Mare reservoir and at the same location Cogolo 2 system receives the contribution from Pian Palù reservoir. In the lower part of the catchment water stored in Santa Giustina and Mollaro reservoirs feeds Taio and Mezzocorona plants, respectively. The inset shows the location of the Noce river basin within the Italian territory.

description of catchment's properties and hydrological processes: the sub-catchment and the channel (Bellin et al., 2015). The former is a portion of the catchment where hillslope processes dominate and the latter is the base element composing the river network that connects the sub-catchments to the control section. Mass balance is applied to each sub-catchment under the assumption that water discharge at its outlet depends nonlinearly upon water storage (Kirchner, 2009; Majone et al., 2010). Subsequently, water discharge in each sub-catchment is routed to the control section by a transfer function which mimics both the delay and storage effects of the channel network.

In the current implementation GEOTRANSF adopts a lumped model formulation aimed at limiting the number of parameters and the computational costs, and in particular it does not include a specific module for glacier dynamics. Snow accumulation and melting are simulated on the basis of a simplified degree-day approach. It is postulated that this simplification does not limit the reliability of the results presented for the case study considered in the present work for the following reasons: i) in a recent analysis the Meteorological Office of the Trentino Province (Meteotrentino, 2011) estimated that glaciarized areas within the Noce river basin totalize a surface of $\sim 18 km^2$, which represents only 1.3% of the total catchment surface; ii) simulations conducted for the future time frame indicated that the total contribution originating from ice melting (i.e., the difference between total cumulated streamflow volume and precipitation) at the Careser control section, immediately downstream the glacier bearing the same name, is, for all the 4 CMs adopted in the present study (see Section 4.1), significantly lower than the mass volume of the Careser

Table 2: Minimum ecological flow ($MEF$) requirements associated to the 5 reservoirs present in the river basin.

| | **Minimum Ecological Flow** [$m^3/s$] | | | | |
|---|---|---|---|---|---|
| | **Before 2003** | **2004-2006**[a] | **2040-2070**[b] | | |
| | | | *Mean* | *Minimum* | *Maximum* |
| *Pian Palù* | 0.0 | 0.10 | 0.18 | 0.14 | 0.21 |
| *Careser* | 0.0 | 0.03 | 0.05 | 0.04 | 0.06 |
| *Malga Mare* | 0.0 | 0.09 | 0.18 | 0.14 | 0.21 |
| *S. Giustina* | 0.0 | 2.10 | 3.24 | 2.63 | 3.68 |
| *Mollaro* | 0.0 | 2.44 | 3.34 | 2.71 | 3.79 |

[a] Constant MEF values adopted during the period 2004-2006. These prescriptions are applicable until the end of 2016 as a consequence of a private agreement between hydropower plant managers and Autonomous Province of Trento.
[b] Monthly variable MEF values adopted for simulations of future periods as prescribed by PGUAP (2006).

glacier, which has been estimated for the year 2006 in $59Mm^3$ (Carturan et al., 2013). However, it is recognized that projected changes in the hydrological cycle and hydropower production at Malga Mare plant may be affected by substantial uncertainty as a consequence of the typically larger uncertainty characterizing high altitude projections of climate models (see the discussion in Sect. 6) and the simplifications introduced by the degree-day model.

GEOTRANSF model was selected because it is specifically designed for addressing the tight coupling between human and natural components of the system. Notice that in addition to hydropower water uses, Noce river basin is intensively exploited with a large number of small water withdrawals (around 2000) for agricultural, civil and industrial uses. It is computationally efficient, thus allowing detailed calibration procedures and simulations extending over long periods.

At a higher hierarchal level the river basin is subdivided into macro-areas, each one identified by an outlet node. In this scheme the nodes are therefore control sections of the river network corresponding to stream gauging stations used in the calibration procedure, reservoirs, or junctions between the river and the artificial channels network for irrigation or withdrawing purposes (see Fig. 1). Water discharge computed at a node can be directly transferred to a downstream node or, in the presence of infrastructures, can be modified through a suitable water balance taking into account the characteristics (i.e., water diversion channel, presence of a reservoir, etc.) and constraints of the licensed water use. Notice that this approach allows flexibility in selecting several control sections within the basin, not necessarily associated with stream-gauging stations.

### 3.1. Model Setup, parameters identification and validation

With the objective to model the alterations in streamflow due to the hydropower systems, the catchment has been divided into 36 macro-areas with 7 nodes used for model calibration. In particular, the control sections adopted for the calibration and validation procedure are located at 4 out of 5 reservoirs considered in the study (Pian Palù, Careser, Malga Mare and S. Giustina) and at 3 stream-gauge stations (Vermiglio, Malè and Mezzolombardo, with the latter being the outlet of the river basin). Each macro-area is characterized by a specific set of 18 parameters, which are listed in Table 3, together with a short explanation of their meaning. Preliminary simulations conducted with a progressive reduction of the number of parameters selected for calibration suggested that 9 out of 18 parameters can be assigned a-priori, while the remaining 9 (see Table 3) should be identified with the help of observational data, which in the present work (and as in most hydrological applications) are limited to the water discharge measurements since state variables, such as soil water content, are not available. Parameters identification is performed by using the classical approach of selecting the combination of parameters that maximize the Nash-Sutcliffe index, which coincides with identifying the maximum of the a posteriori probability density function of the parameters, under the hypothesis that the error is random and Gaussian and that data are not affected by heteroscedasticity (Gelman et al., 1995; Kowalsky et al., 2004):

$$NS = 1 - \frac{\sigma_e^2}{\sigma_0^2} \tag{1}$$

where $\sigma_e^2 = \sum_{j=1}^{N} \left[Q_{c,j} - Q_j\right]^2 /(N-1)$ is the variance of the error, defined as the difference between the computed $Q_{c,j}$ and the measured water discharge $Q_j$ at the control section, $\sigma_0^2 = \sum_{j=1}^{N} \left[Q_j - \overline{Q}\right]^2 /(N-1)$ ] is the variance of

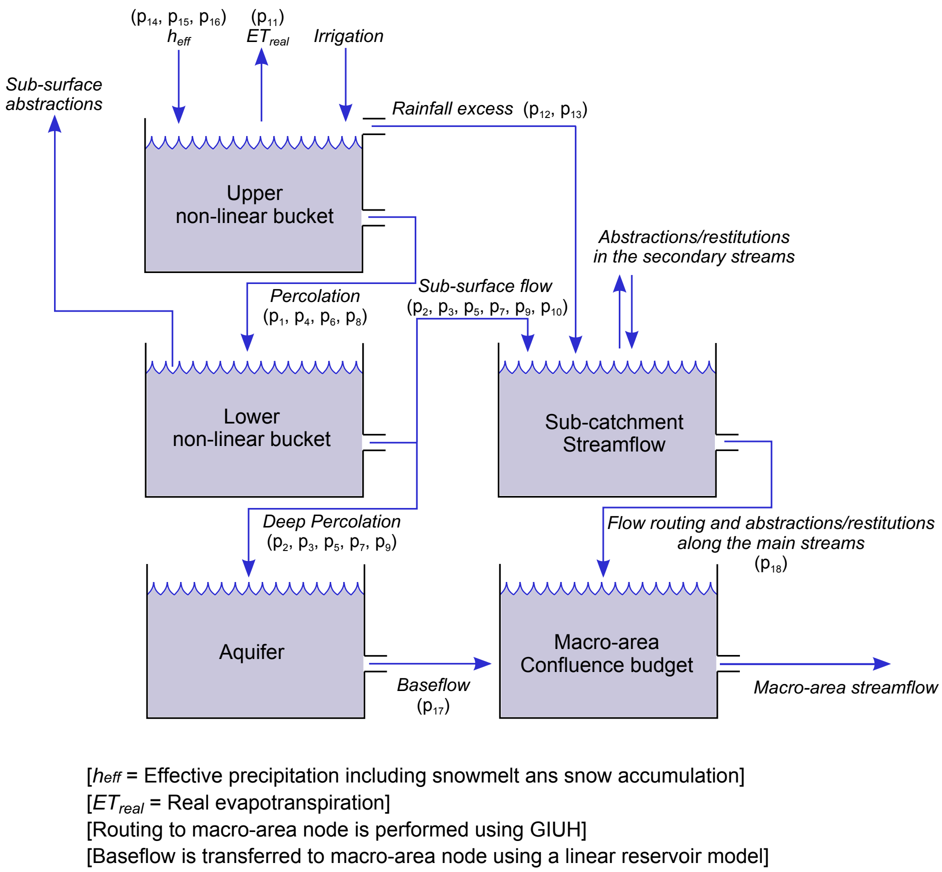


Figure 2: Schematic outline of the main hydrological processes simulated by GEOTRANSF (modified from Bellin et al. 2015). Details on model parameters $p_j$ are provided in Table 3.

the signal, with $\overline{Q} = \sum_{j=1}^{N} Q_j/N$ the mean and $N$ is the number of observations. The parameters space is explored by using the Particle Swarming Optimizer (PSO) (see e.g., Kennedy and Eberhart, 1995), which is particularly effective in finding the optimal point when the number of parameters is large and the objective function is characterized by multiple local maxima (Gill et al., 2006; Castagna and Bellin, 2009). Measured daily water discharges in the period 2000 - 2006 at 7 control sections were used to infer one set of parameters for each macro-area. The year 2000 was used as a spin-up period. Comparisons of observed and predicted streamflows at the seven control sections showed good agreements during the calibration period 2001-2003 with Nash values always larger than 0.69. When applied to the validation period 2004-2006 the optimized parameters provided a good reproduction of the streamflows with NS values slightly smaller than those obtained during calibration (see Table 4). Streamflow regime is significantly altered in 4 out of 7 control sections. In the portion of the catchment contributing to the control section where streamflow is altered the human impact is included.

Outflows from reservoirs as $MEF$, or derived from the reservoir and utilized in the connected hydropower plant were described with simplified operational rules at the monthly time scale. These rules have been inferred from the observational data of the period 2000-2006. Constant daily water discharges equal to the monthly mean values of the period 2000-2006 were considered as management rule of the reservoirs, by assuming that the hydropower plants does not produce during the weekends, when the price of energy is typically low, except when the reservoir reaches the maximum operational level. In addition, water in the reservoirs may oscillate between a maximum and minimum operational level, according to the specific protocols enforced by river authority to preserve $MEF$ (see Table 2). This deterministic model of water releases is similar to the approach adopted by Schaefli et al. (2007), with

Table 3: GEOTRANSF model parameters. Symbols "✓" and "-" indicate if the parameter has been calibrated or fixed to a given value, respectively.

| Description | Symbol | Model Component | Calibration |
|---|---|---|---|
| sub-surface flow variation rate (layer 1) | $p_1$ | sub-surface flow | ✓ |
| sub-surface flow variation rate (layer 2) | $p_2$ | sub-surface flow | - |
| sub-surface flow partition coefficient (layer 2) | $p_3$ | sub-surface flow | ✓ |
| soil depth (layer 1) | $p_4$ | sub-surface flow | - |
| soil depth (layer 2) | $p_5$ | sub-surface flow | ✓ |
| residual water content (layer 1) | $p_6$ | sub-surface flow | - |
| residual water content (layer 2) | $p_7$ | sub-surface flow | - |
| specific water flux (layer 1) | $p_8$ | sub-surface flow | - |
| specific water flux (layer 2) | $p_9$ | sub-surface flow | - |
| maximum specific flux (layer 2) | $p_{10}$ | sub-surface flow | - |
| parameter controlling water stress reduction factor | $p_{11}$ | evapotranspiration | ✓ |
| multiplicative coefficient for threshold parameter triggering runoff | $p_{12}$ | rainfall excess | ✓ |
| multiplicative coefficient for maximum infiltration capacity | $p_{13}$ | rainfall excess | ✓ |
| threshold temperature below which precipitation is always solid | $p_{14}$ | snow | ✓ |
| threshold temperature above which melting occurs | $p_{15}$ | snow | ✓ |
| melting factor | $p_{16}$ | snow | ✓ |
| linear reservoir constant | $p_{17}$ | baseflow | - |
| parameter controlling streamflow velocity | $p_{18}$ | GIUH routing | - |

the difference that, given the type of available data, variability at scales smaller than the monthly scale are neglected. Notice that $MEF$ monthly releases were introduced only after 2003, the year in which $MEF$ prescriptions have been enforced (PGUAP, 2006). For a detailed description of the calibration of the GEOTRANSF modeling framework (i.e., hydrological modeling and reservoir operations) to the Noce river basin we refer to Bellin et al. (2015).

Table 4: $NS$ index during calibration and validation periods for the 7 control sections within the catchment.

| | Pian Palù | Careser | Malga Mare | Vermiglio | Malè | S. Giustina | Mezzolombardo |
|---|---|---|---|---|---|---|---|
| *NS cal* | 0.84 | 0.78 | 0.76 | 0.69 | 0.93 | 0.84 | 0.94 |
| *Ns val* | 0.72 | 0.63 | 0.72 | 0.69 | 0.91 | 0.76 | 0.95 |

## 4. Climate change projections

### *4.1. Climate models, bias-correction and downscaling*

Climate forcing applied in this study was selected and preprocessed during a preliminary auditing and intercomparison activity described in Deidda et al. (2013), which was conducted within the framework of the FP7 CLIMB (Climate Induced Changes on the Hydrology of Mediterranean Basins; http://www.climb-fp7.eu) project (Ludwig et al., 2010). Such a prior analysis was focused on 14 Climate Models (CMs) runs, which were obtained by combinations of a number of nested Global and Regional Climate Models (GCMs and RCMs) under the SRES A1B scenario (IPCC SRES, 2000) and made available through a policy of open access output by the FP6 ENSEMBLES project (http://ensembles-eu.metoffice.com).

The preliminary analysis was addressed to evaluate the performances of the 14 CMs in reproducing the precipitation and temperature climatologies on selected basins of the Mediterranean area (including the Noce), with the aim to choose a common subset of best performing CMs across all the considered basins and to make inter-regional analyses and intercomparisons of likely climate change impacts. To pursue this objective, the E-OBS dataset (Haylock et al., 2008) was used as a common reference, with the advantage of using a standard product regardless of the target basin, and the drawback related to local inaccuracies of the estimation arising from the density of the station network adopted for producing the dataset. A subset of 4 best performing CMs were then selected on the basis of their score in reproducing certain metrics (describing model's capability to reproduce the seasonal mean and variability of precipitation and temperature) across all the considered basins, and with the additional constraint to include at least two different driving GCMs and two different nested RCMs to retain a minimum information on intermodel uncertainty, as described in Deidda et al. (2013). The 4 selected CMs are listed in the following with their acronyms, which refer to the corresponding driving GCM (first three characters) and nested RCM (last three characters), respectively: i) 'HCH-RCA'= HadCM3 - High Sensitivity (UK) driving RCA (Sweden); ii) 'ECH-RMO'= ECHAM5/MPI (Germany) driving RACMO2 (Netherlands); iii) 'ECH-REM'= ECHAM5/MPI (Germany) driving REMO (Germany); vi) 'ECH-RCA'= ECHAM5/MPI (Germany) driving RCA (Sweden). For details on the auditing process that leaded to this subset of 4 CMs, the reader is referred to Deidda et al. (2013). It is also worth mentioning that the ensemble of the 4 CMs selected in the present study does not fully explore all the uncertainties associated to climate model selection, nor it considers the full range of emissions scenarios or the effect of different starting initial conditions. The selection of the CMs adopted represents an "ensemble of opportunity" (in the sense introduced by Tebaldi and Knutti, 2007) with the size determined to some degree for pragmatic reasons.

ENSEMBLES CMs provided continuous gridded time series of daily precipitation and temperature from 1950 to 2100 at a resolution of about 25 km. However, these outputs cannot be directly applied as forcing of hydrological models, because CMs are affected by well known biases and the resolution is too coarse to properly account for small scale variability and local orographic conditioning. As an example, Figure 3a compares the seasonal variability of precipitation for the 14 CMs considered in Deidda et al. (2013) and E-OBS in terms of monthly means for a 60-year period (1951-2010) over a 4x4 grid stencil centred in the Noce basin. This figure clearly shows a large spread among the CMs and also some discrepancies with respect to E-OBS. For instance, large differences in monthly precipitation totals and seasonality can be observed, as already discussed in the Introduction. Some discrepancies affect also the temperature signals, as shown in Figure 3b, where an intermodel spread larger than 5 K in monthly mean temperature is observed, as well as different ranges between summer and winter monthly mean temperature. Another problematic issue is related to the coarse spatial resolution of CMs and concerns the reliable representation of local features and observed spatial variability, as shown in Figure 4, where average annual values of precipitation and temperature of the period 1970 - 2000 were reconstructed by GEOTRANSF preprocessing module, for each one of 328 Noce sub-catchments. The reconstruction was performed starting from time series of daily precipitation and temperature at 28 meteorological stations provided by Meteorological office of the Province of Trento (MeteoTrentino, http://www.meteotrentino.it).

In order to deal with the discrepancies summarized in Figure 3 and to proper account for local climatology and orographic effects, as those depicted in Figure 4, bias-correction and downscaling techniques were applied to precipitation and temperature fields of the 4 selected CMs, making them suitable as GEOTRANSF input forcing. Specifically, E-OBS were used as reference for large scale corrections while local stations (OBS) assured a reliable reproduction of local features at the catchment scale.

Bias-correction techniques were thus first applied to CMs precipitation and temperature fields using empirical quantile-quantile transformations able to reproduce the shape of the distribution and a reliable seasonal variability (see e.g., Berg et al., 2012; Teutschbein and Seibert, 2012). Moreover, precipitation fields were downscaled from 25-km to 1-km resolution regular grid using the Space-Time RAINfall model (STRAIN) described in Deidda (2000), whose performance were successfully tested in several contexts (e.g., Deidda et al., 2004, 2006), and a modulation function was then applied to account for the orographic effects, as described in Badas et al. (2006). Temperature fields were instead interpolated at 1 km resolution using a Barnes technique (Barnes, 1964, 1973) and a time-varying lapse-rate, as described in Liston and Elder (2006), to proper account for the different elevations among CMs orography, measuring stations, and the final 1-km resolution digital terrain model. Finally, 1-km resolution downscaled time series of temperature and precipitation were assigned to the 328 Noce sub-catchments by applying belonging or proximity criteria.

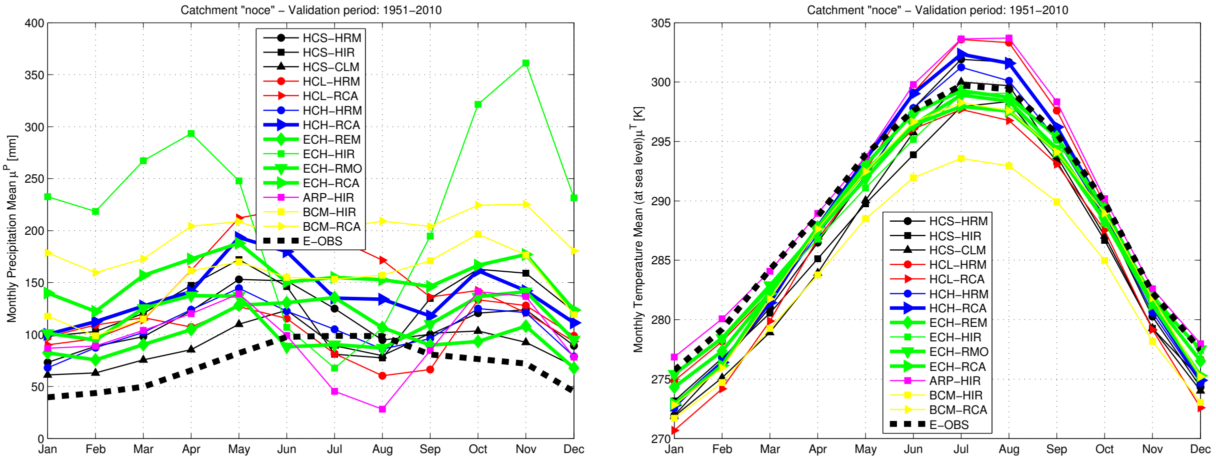


(a) (b)

Figure 3: Mean monthly precipitation (a) and temperature (b) over the 60-yr period (1951-2010) for the 14 ENSEMBLES models and E-OBS dataset. Results are based on areal averages over a 4×4 grid-point stencil centered in the Noce catchment. The reader is referred to Deidda et al. (2013) for more details on models and acronyms.

### *4.2. Trend of precipitation and temperature projections*

Although the analyses that will be discussed in the ensuing sections will focus on the the bias-corrected and downscaled/interpolated outputs of the 4 selected CMs considering both a reference (REF, 1970-2000) and a future (FUT, 2040-2070) period, it is also interesting to investigate the trend of precipitation and temperature projections along a wider time-frame and considering large scale raw data from all 14 ENSEMBLES CMs. To this end five 30-yr climatological periods between 1951 and 2100 are considered with precipitation and temperature averages calculated in each 30-yr period over a 4×4 grid-point stencil (about 100×100 square km) centred in the Noce catchment. Figure 5 shows the differences for each period with respect to the first one (1951-1980). All CMs coherently indicate a positive trend in future temperature projections, although the size of the increment varies from model to model, as shown by Figure 5b. Conversely, for precipitation (Figure 5a), contradicting trends among different CMs are observed, some of them indicating a large scale precipitation increase, while others suggesting a decrease. Moreover, some CMs show alternation of positive and negative trends between consecutive periods. Both these aspects clearly indicate the large uncertainty which is related to the assessment of future precipitation projections in the GAR, as also observed by other authors (see Introduction).

Indeed, refining our analyses on bias-corrected and downscaled/interpolated fields pertaining to the Noce basin (as described in previous Section 4.1), similar behaviors and similar uncertainties can be observed, which will be further reflected into the projections of hydrological response of the catchment and hydropower production (see ensuing Sections). Figure 6 shows catchment-averaged monthly values of temperature and precipitation during REF (1970-2000) and FUT (2040-2070) periods for the 4 selected CMs, while Table 5 summarizes the annual and seasonal changes for each CM. Looking at temperatures (Figure 6b) a projected increase of about 2 K for all the models is observed, except for HCH-RCA which predicts a larger temperature increase of about 4 K. It is also worth noticing that projected changes in temperature from each CM is quite constant along the year, regardless of the season. Conversely, interpretation of trend and monthly distribution of precipitation (Figure 6a, Table 5) is again problematic and uncertain. There is a slight increase in annual precipitation totals, varying from 2% to 6% depending on the model, while looking at seasonal and monthly variations a general agreement among CMs is observed, with few discrepancies: all the models exhibit an increase in winter (ranging from 12 to 46%), a slight decrease in spring and summer, and a further increase in autumn (varying between about 3 and 12 % depending on the model) with a peak in October, except for HCH-RCA. However, as already discussed in the Introduction, determination of precipitation trends in the GAR is a difficult task and often fraught of uncertainty. In addition, while for temperature no significant spatial dependence was detected, for precipitation signal changes were more marked in those sub-catchments with higher elevations (figures

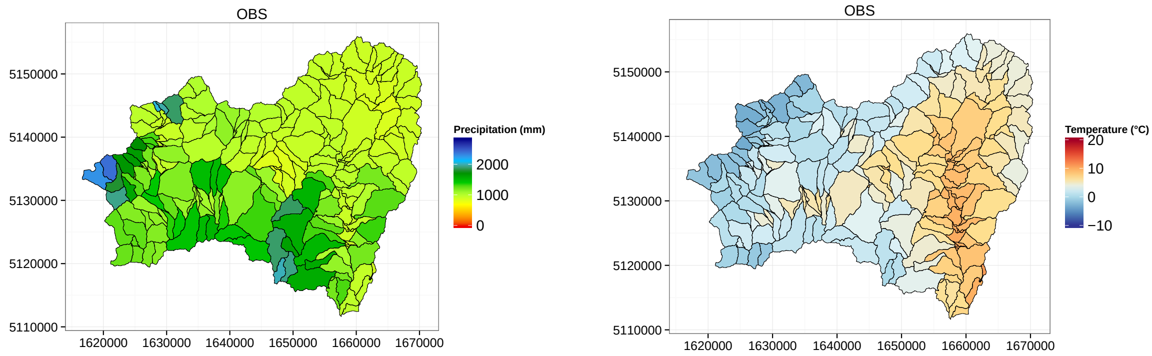


(a) (b)

Figure 4: Spatial distribution of observed (OBS) average annual (a) precipitation and (b) temperature during the period 1970-2000.

Table 5: Catchment-averaged temperature ($^\circ K$) and precipitation (%) for the Bias-Corrected CM simulations during the period 2040-2070. Values in brackets denote percentage deviation (for precipitation) and absolute change (for temperature) from the associated CM REF simulation. Catchment-averaged values for observed (OBS) dataset are also presented.

| **Temperature** [$^\circ K$] | *Winter* | *Spring* | *Summer* | *Autumn* | *Annual* |
|---|---|---|---|---|---|
| **ECH-RCA (2040-2070)** | 0.1 (2.4) | 8.6 (2.3) | 14.1 (2.8) | 2.8 (2.0) | 6.4 (2.4) |
| **ECH-REM (2040-2070)** | -0.3 (2.1) | 8.1 (1.9) | 13.8 (2.5) | 2.7 (2.1) | 6.1 (2.2) |
| **ECH-RMO (2040-2070)** | -0.6 (1.9) | 8.5 (2.2) | 13.6 (2.3) | 2.5 (1.7) | 6.0 (2.0) |
| **HCH-RCA (2040-2070)** | 1.4 (4.2) | 10.3 (4.4) | 15.2 (4.4) | 3.9 (3.5) | 7.7 (4.1) |
| **OBS (1970-2000)** | -2.5 | 6.2 | 11.2 | 0.7 | 3.9 |

| **Precipitation** [$mm$] | *Winter* | *Spring* | *Summer* | *Autumn* | *Annual* |
|---|---|---|---|---|---|
| **ECH-RCA (2040-2070)** | 258.9 (21.9%) | 345.8 (-2.3%) | 329.8 (0.2%) | 338.8 (11.8%) | 1273.4 (6.2%) |
| **ECH-REM (2040-2070)** | 237.8 (12.2%) | 330.5 (-3.3%) | 336.5 (2.8%) | 311.8 (5.3%) | 1216.5 (3.4%) |
| **ECH-RMO (2040-2070)** | 256.4 (21.7%) | 328.8 (-3.1%) | 300.3 (-7.1%) | 313.0 (3.7%) | 1198.5 (2.0%) |
| **HCH-RCA (2040-2070)** | 261.6 (46.0%) | 342.5 (-0.7%) | 307.9 (-9.3%) | 278.2 (-3.6%) | 1190.2 (3.3%) |
| **OBS (1970-2000)** | 195.9 | 330.0 | 310.4 | 279.5 | 1172.3 |

not shown).

## 5. Validation under the REF scenario (1970-2000)

The parameters identified by maximizing the NS index on the calibration period (2001-2006), as described in Section 3.1, were used to simulate, through a forward application of the model, the streamflow in the REF period 1970-2000, with measured precipitation and air temperature as input meteorological forcing (see Section 4). Unfortunately, daily operations on the reservoirs were not available for this period, and therefore mean operational rules, as inferred for the period 2000-2006, where used to approximate water transfers from reservoirs to the connected hydropower plants (Bellin et al., 2015). Notice that $MEF$ was not imposed during the REF period. Similarly to the calibration procedure, the first year of the time series (1970) was used as spin-up for the hydrological simulations and was not used in the computation of the $NS$ index.

The only stream-gauge with a long water discharge time series within the REF period is Malé, with observations available during the period 01/05/1988 - 31/12/2000. A scatterplot of daily simulated and observed water discharge data at Malé is presented in Fig. 7a and resulted in a Nash-Sutcliffe index of $NS = 0.79$. Points are grouped

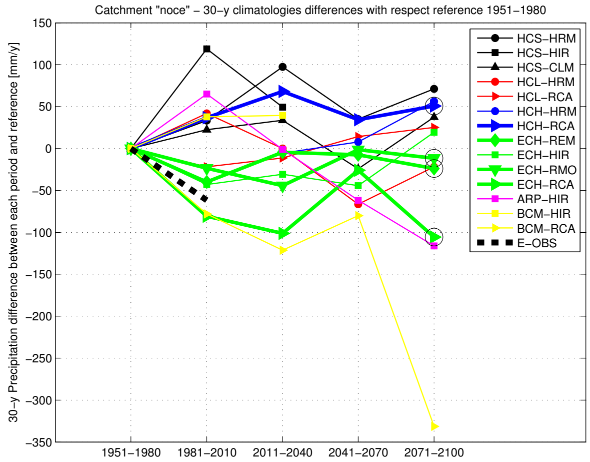


(a)

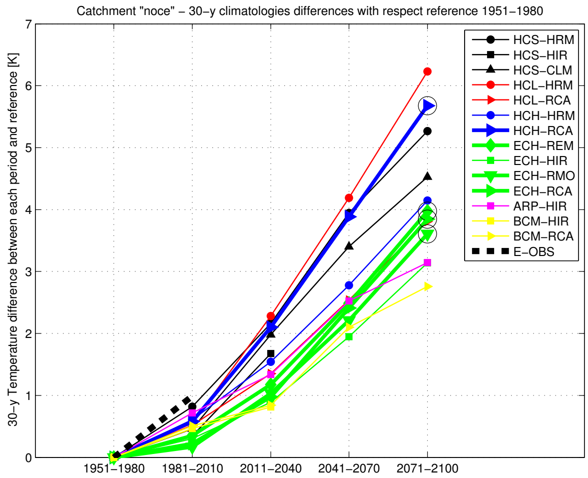


(b)

Figure 5: Averages of precipitation (a) and temperature (b) fields from the 14 ENSEMBLES models over five 30-yr non-overlapping climatological periods between 1951 and 2100. Results are based on areal averages over a 4×4 grid-point stencil centered in the Noce catchment and are presented in terms of differences between the average in each period with respect to the average in the first period (1951-1980). The reader is referred to Deidda et al. (2013) for more details on models and acronyms.

symmetrically around the 1:1 line thus indicating that the model does not introduce bias in the simulations. Visual inspection of the comparison between simulated and observed water discharge for the years 1997 and 1999 (right side of Fig. 7a) further confirms that the model provides a good reproduction of observed water discharge in the reference period. Notice that in the calculation of $NS$ the period 01/08/1991 - 31/12/1994 was excluded due to unreliable observed water discharge data. Flow duration curves (FDCs) have been also used to assess differences in the probability distribution at low, intermediate and high flows between simulated and observed water discharge under the REF scenario. Following Yilmaz et al. (2008) and Majone et al. (2012) low flows are identified as those with a probability of exceedance larger than 0.7, intermediate flows as those with probability of exceedance in the range 0.2-0.7 and high flows as those with probability of exceedance smaller than 0.2. Fig. 7b compares FDCs for observed and simulated daily water discharge at Malé in the periods 01/05/1988 - 31/07/1991 and 01/01/1995 - 31/12/2000. The simulated FDC overestimates the observed FDC at low flows, but the match improves significantly at intermediate to high flows. These differences are most likely due to changes in the management of the reservoir with respect to the mean operational rules inferred from the data, which by definition neglect intra-annual modifications of reservoirs management.

GEOTRANSF was then run in the REF period with bias-corrected and downscaled CM forcing, again with the same parameters identified as described in Section 3.1, in order to verify whether CM REF simulations applied as meteorological forcing to the hydrological model are compatible, in statistical terms, with the water discharges simulated using OBS forcing (see Fig. 7c). Figure 7c clearly shows that CMs are able to reproduce fairly well the FDC when used in the hydrological model instead of the observed precipitations and temperatures. These results show that CM simulations produce in the REF period a meteorological forcing compatible with the observed water discharge at Malé and thus can be safely adopted for the impact assessment that will be presented in the ensuing Sections. In particular, the projections in the FUT period resulting from the 4 bias-corrected and downscaled CM outputs adopted in this study will be compared on a CM by CM basis with the results of the hydrological simulations of the REF period forced by bias-corrected and downscaled CM forcing.

## 6. Impacts on hydrological cycle

Here the impact of climate change on water resources in the Noce catchment is investigated with reference to the REF (1970-2000) and FUT (2040-2070) scenarios. Hydrological simulations, using GEOTRANSF, were conducted

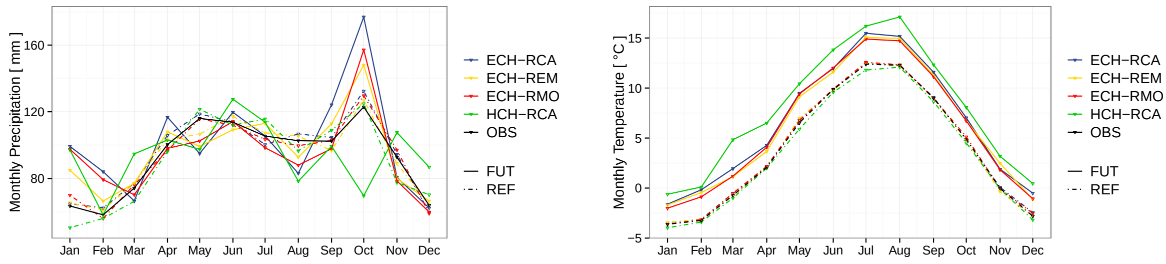


(a) (b)

Figure 6: Catchment-averaged monthly values of (a) mean precipitation and (b) temperature for the Noce river basin under the the REF and FUT scenarios. Monthly values obtained by using the observed precipitation and temperature time series (OBS) are shown with a solid black line.

for both scenarios using parameters calibrated on the period 2001-2006 and the management rules, including $MEF$ prescriptions only for the FUT period, for the 5 reservoirs as provided by Bellin et al. (2015). Notice that for both REF and FUT time slices the first year of simulation (i.e., 1970 and 2040) has been used a spin-up period.

Although all CM simulations indicate a significant increase in winter precipitation (see Table 5), the simultaneous increase of winter temperature (about 1.9 to 4.2 K) results in a significant reduction of catchment-averaged Snow Water Equivalent (SWE) in the range between -68% and -90% on the annual basis. SWE reductions are, for each CM simulation, almost homogeneous throughout the year, with a slightly higher reduction in the range between -74% and -92% observed in summer. In absolute terms the effect of temperature rising is thus stronger than the effect of precipitation increase and as a consequence much of precipitation shifts from snow to rainfall and snow-cover season shortens (see e.g., Farinotti et al., 2012). The projected changes in SWE for the Noce catchment is in line with the recent findings of Laghari et al. (2012) which observed in the Austrian Alps an annual average SWE reduction ranging from -50% to -96%.

As a consequence of warmer temperatures and increased precipitation, the seasonal runoff (i.e. the sum of baseflow, sub-surface flow and direct runoff without taking into account flow routing and water abstractions/restitution) generation dynamics will significantly change in the Noce catchment. Less winter precipitation falling as snow and the melting of winter snow occurring earlier in spring, with respect to the REF period, will lead to a shift in the runoff regime with the peak decreasing in maximum intensity and anticipating from July to June (see Fig. 8). On annual basis, catchment-averaged runoff is projected to increase in the range 5% (ECH-RMO) to 14% (ECH-RCA) as a consequence of the increased precipitation and a limited rise of evapotranspiration (average annual increase among all the 4 CMs of the order of $\sim 25\,mm$). During winter, a significant increase, between 30% and 81%, of runoff is projected in the FUT scenario. The largest increase of about $75mm$ during winter is associated to HCH-RCA, which is the ensemble member presenting the largest increase in precipitation and temperature during winter season (see Table 5). Runoff is projected to increase also in spring (between 12% and 35%) and fall (between 10% and 24% in 3 out of 4 CMs, with only HCH-RCA presenting a decrease of -3%), showing in the latter case a possible vulnerability of the catchment to flood events in fall. Summer runoff is projected to decrease in the range between -11% and -23% in a period characterized by high runoff. An anticipated and attenuated summer peak, with respect to the REF scenario, caused by the smaller contribution from a dwindling winter snow-pack, is indicative of a transition of the catchment from a glacio-nival to a nival regime (Farinotti et al., 2012) and is in line with recent investigations conducted in the Alpine region (Jasper et al., 2004; Finger et al., 2012; Laghari et al., 2012; Bavay et al., 2013).

Fig. 9 shows the projected variation of monthly water discharge simulated at 4 nodes (Vermiglio, Malé, S. Giustina and Mezzolombardo, see Fig. 1) located from upstream to downstream along the Noce main reach. Simulated changes in water discharge at 3 locations present a shift in the annual peak, which anticipates from July to June (Figs. 9a, b and c). However, Mezzolombardo (Fig. 9d) shows a different behavior with summer water discharge peak being in July for both REF and FUT scenarios. This occurrence is caused by the Santa Giustina and Mollaro reservoirs in the middle course of the Noce, which exert a significant alteration of streamflow, which reflects also to the seasonal

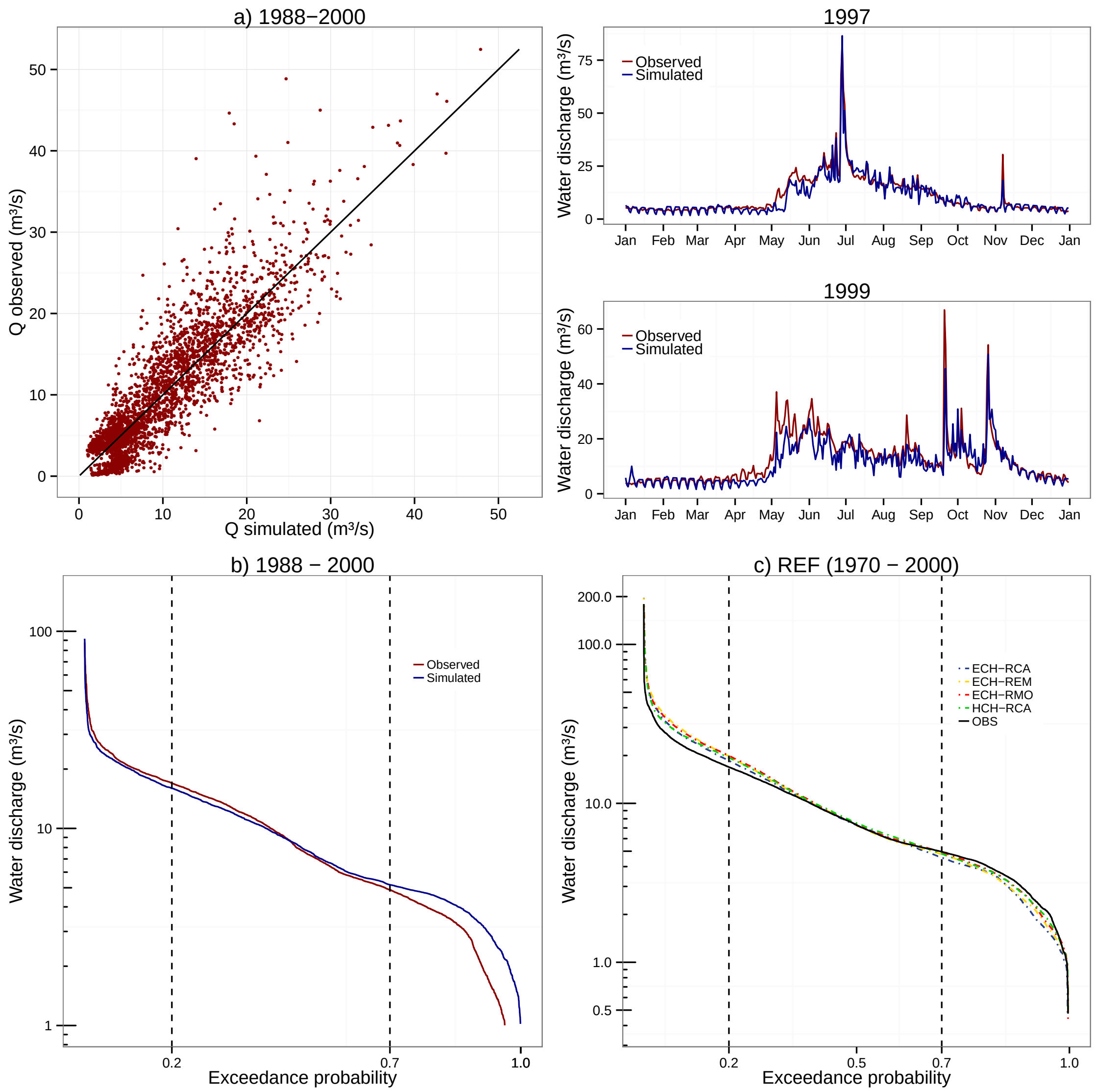


Figure 7: Daily water discharge simulated by GEOTRANSF at Malé node. For the "validation" period 1988-2000, comparison of observed and simulated daily water discharges (using observed precipitation and temperature time series as external forcing): panel a) on left-hand side, scatterplot of observed vs simulated values, on the right-hand side, details on time series comparisons for 1997 and 1999 years; panel b) FDCs for observed (red line) and simulated values (blue line). Panel c) for the "reference" (REF) period 1970-2000, comparison of FDCs for water discharge simulated by GEOTRANSF using as forcing precipitation and temperature from bias-corrected and downscaled CMs (color dashed lines) and from instrumental time-series (continuous black line). Vertical dashed lines in b) and c) divide the curves into three portions corresponding to high, medium and low flows, respectively.

means. In general, the percentage increase in streamflow projected for the FUT scenario is larger in headwaters upstream of the Malé gauging station, which reflects the largest projected increase of precipitation in headwaters. Changes in streamflow are smaller in the middle and lower portions of the catchment, due to the mild change in the climatic forcing, with respect to the upper part, and the significant alteration due to the S. Giustina reservoir. This can be clearly seen in Table 6. Despite the fact that Vermiglio is the gauging station at the highest altitude within the catchment, the projected increase (between 7% and 13%) is comparable with that of Mezzolombardo (between 6% and 14%) as a consequence of the projected variations in precipitation which indicate, for the drainage area associated

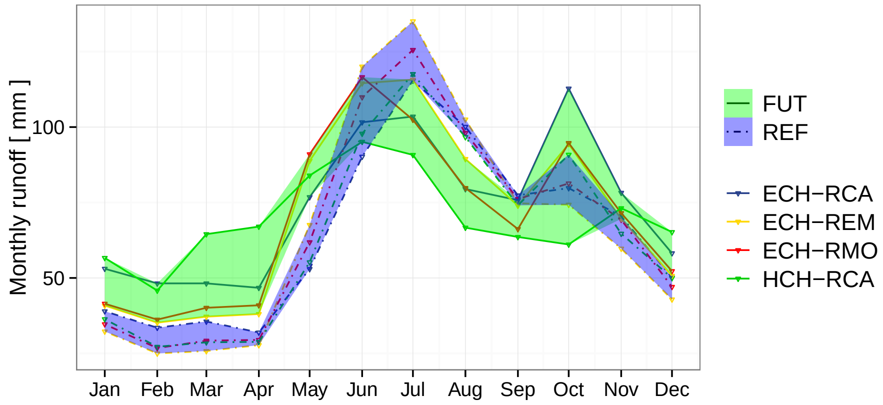


Figure 8: Catchment-averaged monthly runoff (mm/month) values for the Noce river basin under REF and FUT scenarios. Shaded area indicate the CMs envelope for the respective periods.

to Vermiglio, significantly lower changes with respect to the North-western part of the catchment.

Simulated daily FDCs at Vermiglio, Malé, S. Giustina and Mezzolombardo are shown in Fig. 10 for both the REF and FUT time slices. Duration curves based on simulated water discharge with CM REF climatic forcing are barely distinguishable one to each other, thereby confirming that the adopted bias-correction and downscaling techniques reproduce correctly the characteristics of the climate in the REF period. Simulations for the FUT scenario show an upward shift in the FDCs at all locations. Differences in high flow regimes between REF and FUT simulations are small to negligible supporting the idea that projected changes in meteorological forcing for the Noce river basin under a medium-term scenario will not introduce significant changes in the magnitude and frequency of high flow regime. However, at all locations all CMs project a general increased frequency of medium and low flows with respect to REF simulations. At Vermiglio, Malé and S. Giustina the increase is relatively higher for low flows than for medium flows, whilst at Mezzolombardo the deviation are concentrated in the medium flows range. Notice that the projected increases at medium and low flows are in agreement with the expected changes in the seasonal distribution of runoff (see Fig. 8 and the discussion above) which showed pronounced changes during periods characterized by low flow conditions (i.e. the winter months). As already highlighted the magnitude of the changes is local and in general they are more pronounced at higher altitudes. Simulated FDCs at Mezzolombardo for both REF and FUT scenarios show a step-wise behavior essentially due to the use of simplified operation rules at the S. Giustina and Mollaro reservoirs, which assume a target monthly value of diverted flow to the connected hydropower plants. Furthermore, at low flows and for both scenarios FDCs are steeper than in the other locations indicating an higher level of variability in the water discharge regime exerted by the two reservoirs. Interestingly, the increased length of the plateau at $\sim 70m^3/s$ under the FUT simulations reveals that the percentage of time in which water diverted from S. Giustina reservoir will be equal to the maximum flow capacity (i.e., $66m^3/s$, see Table 1) will increase by $\sim 6-7\%$.

## 7. Impacts on hydropower potential

Changes in the hydropower potential, defined as the energy that may be produced by the hydropower plant, given a water yield, provide a solid indication of the impact of climate change on hydropower production. In the present work the Technical Hydropower Potential (THP) (see e.g., Kumar et al., 2011; Hamududu and Killingtveit, 2012; Gaudard and Romerio, 2014) is adopted as a metric of comparison among alternative scenarios, which is defined as the maximum amount of energy that can be produced in a given period of time by assuming maximum efficiency of the system and independently from economic and other restrictions. The technical potential is often used as a reference since the economic potential, defined as the "portion of the technical potential which can be developed at costs competitive with other energy sources" (Gaudard and Romerio, 2014), fluctuates according to energy market

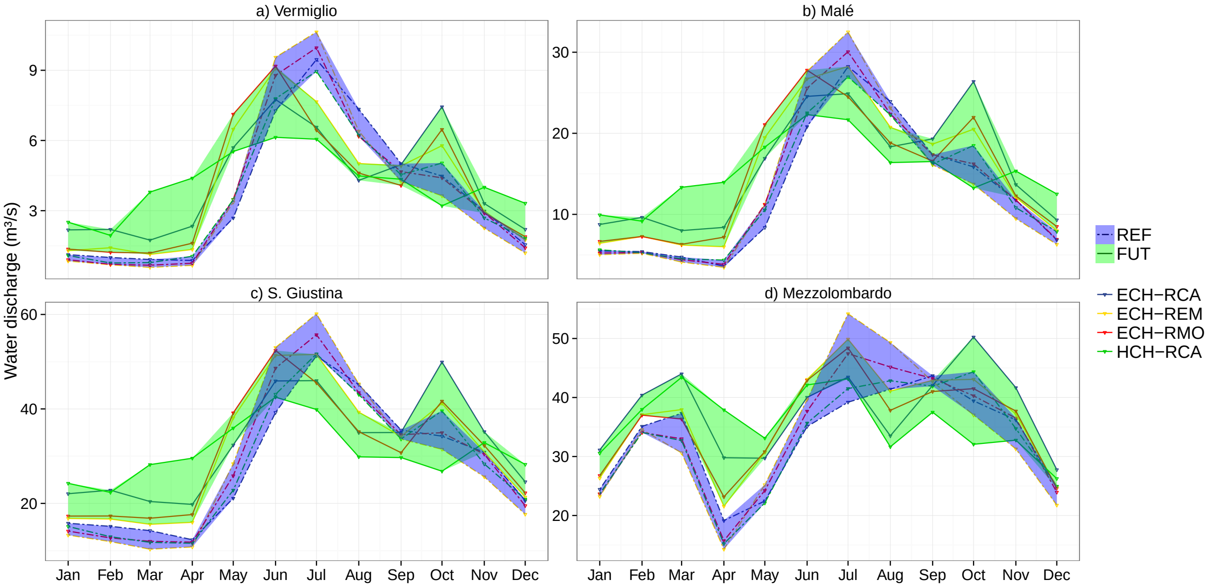


Figure 9: Projected changes in monthly water discharge at Vermiglio, Malé, S. Giustina and Mezzolombardo locations for the REF and FUT scenarios. Shaded area indicate the CMs envelope for the respective periods.

and is influenced by energy policies, such as the special incentives introduced by the EU to reduce the dependence from fossil fuels. THP for a given hydropower plant during a time period $\Delta t$ is then defined as:

$$THP = \rho g \int_0^{\Delta t} Q(t)\ H(t)\ \eta(t) dt \tag{2}$$

Table 6: Simulated average daily water discharge at Vermiglio, Malé, S. Giustina and Mezzolombardo nodes for the REF and FUT scenarios. Averages for FUT scenario are expressed in terms of percentage anomalies with respect to the associated CM REF simulation.

| | **ECH-RCA** | | **ECH-REM** | | **ECH-RMO** | | **HCH-RCA** | |
|---|---|---|---|---|---|---|---|---|
| | **REF** $(m^3/s)$ | **FUT** [%] | **REF** $(m^3/s)$ | **FUT** [%] | **REF** $(m^3/s)$ | **FUT** [%] | **REF** $(m^3/s)$ | **FUT** [%] |
| *Vermiglio* | 3.74 | 13.2 | 3.69 | 10.7 | 3.75 | 7.1 | 3.70 | 12.2 |
| *Malé* | 12.75 | 23.3 | 13.20 | 14.2 | 13.41 | 11.6 | 13.01 | 17.2 |
| *S. Giustina* | 28.03 | 15.8 | 28.56 | 9.1 | 28.73 | 7.1 | 27.97 | 10.4 |
| *Mezzolombardo* | 33.18 | 13.8 | 33.66 | 7.8 | 33.75 | 5.6 | 32.81 | 8.7 |

where $\rho$ is the density of water, assumed constant in time, $g$ is the gravitational acceleration, $Q$ is the flow rate elaborated by the turbine, $H$ is the gross hydraulic head, which definition depends on the type of turbine, and $\eta$ is the efficiency coefficient for turbines and generators. In the forthcoming calculations the following assumptions are made: i) $H$ is varying in time as simulated by reservoir management rules, but losses in the hydraulic components (power canal, head-race tunnels and penstocks) leading water to the turbine are neglected; ii) $\eta$ is assumed constant in time and equal to 1; iii) THP is constrained by site-specific local regulations on flood protection and minimum ecological flow (see Table 2), which are defined in the Water Uses General Act of the Province of Trento (PGUAP, 2006); iv) if the storage capacity of the reservoir is reached spilling water in not accounted for hydropower production; v) Eq. (2) is integrated with a daily time step during which flow rate and gross head are assumed constant as simulated by hydrological and reservoir modules.

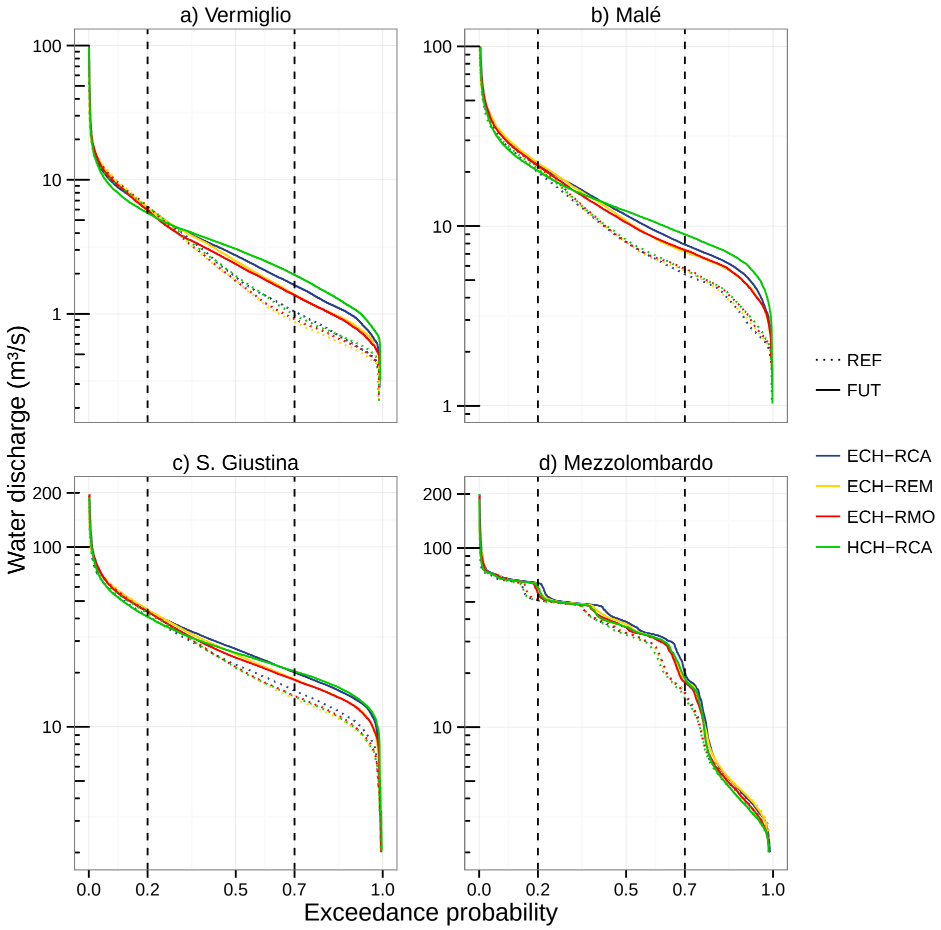


Figure 10: Simulated daily FDCs calculated at a) Vermiglio, b) Malé, c) S. Giustina and d) Mezzolombardo for the four different CMs adopted in the study during under REF and FUT scenarios, respectively. Vertical dashed black lines divide the curves into three portions corresponding to high flows (0-20%), medium flows (20-70%), and low flows (70-100%). Water discharge is plotted on a log scale which emphasizes differences in low flows.

In order to separate the effects on THP due to climate change from local water policies a new operating scenario has been elaborated. In this scenario, hereafter referred to as FUT CC, the reservoir-specific prescriptions in term of $MEF$ are removed for the 2040-2070 time frame, such that releases from the reservoirs and in stream intake structures are as in the REF scenario. Specifically, under FUT CC scenario all the incoming flow in the reservoirs can be used in the hydropower plant with the only limitation represented by the maximum flow capacity of the head race tunnels.

The projected change of the average daily flow passing through the tailrace to reach the powerhouse (see Table 7) is considered as a first indicator of the impact of climate change on hydropower production. Flows are calculated for each CM as the average of the 30 years time frames. Under FUT CC scenario the percentage increase of the usable streamflow is higher in the upper course than in the middle course reservoirs. Moving from higher to lower altitudes, changes are in the range between 59% and 203% for Careser, between 47% and 106% for Malga Mare, between -3% and 13% for Pian Palù, between 7% and 14% for S. Giustina and between 7% and 13% for Mollaro, respectively, depending on the considered CM. High percentage changes at Careser and Malga Mare are however associated to relatively small fluxes in comparison to the other power plants under the REF scenario. This result

Table 7: Simulated average daily diverted flows from the reservoirs. CM averages for FUT CC and FUT scenarios are expressed in terms of percentage anomalies with respect to the associated CM REF simulation.

| **Model** | ECH-RCA | | | ECH-REM | | | ECH-RMO | | | HCH-RCA | | |
|---|---|---|---|---|---|---|---|---|---|---|---|---|
| **Period** | *REF [GWh]* | *FUT CC [%]* | *FUT [%]* | *REF [GWh]* | *FUT CC [%]* | *FUT [%]* | *REF [GWh]* | *FUT CC [%]* | *FUT [%]* | *REF [GWh]* | *FUT CC [%]* | *FUT [%]* |
| *Pian Palù* | 1.73 | 13.4 | 4.1 | 1.77 | 4.7 | -4.5 | 1.80 | 0.2 | -8.6 | 1.78 | -2.8 | -12.2 |
| *Careser* | 0.27 | 203.4 | 184.6 | 0.49 | 64.5 | 54.2 | 0.50 | 58.6 | 48.6 | 0.42 | 106.6 | 94.7 |
| *Malga Mare* | 1.08 | 106.2 | 91.4 | 1.50 | 50.2 | 39.8 | 1.54 | 46.8 | 36.5 | 1.39 | 97.7 | 86.9 |
| *S. Giustina* | 27.69 | 13.8 | 3.0 | 28.13 | 8.7 | -2.1 | 28.15 | 6.9 | -3.6 | 27.61 | 10.3 | -1.1 |
| *Mollaro* | 27.64 | 13.3 | 2.6 | 27.94 | 8.8 | -2.0 | 27.96 | 6.9 | -3.5 | 27.49 | 10.3 | -1.1 |

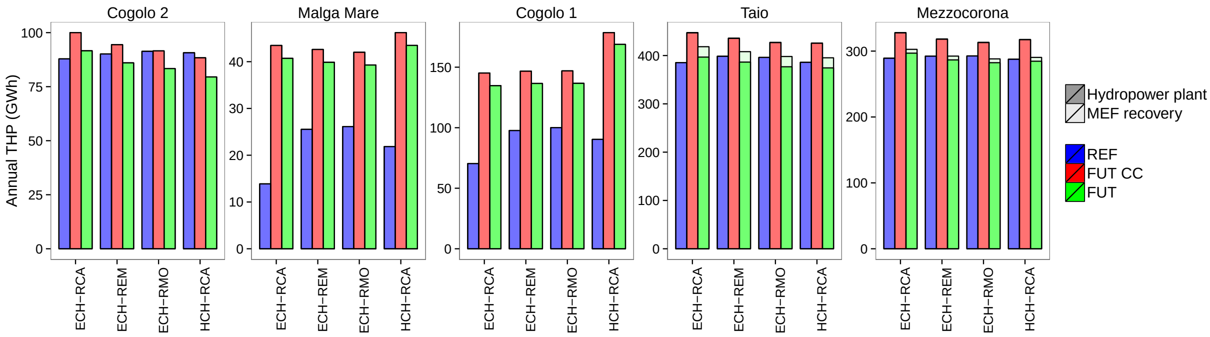


Figure 11: Average annual Technical Hydropower Potential (THP) for each of the 5 powerplants considered in the present study with reference to REF, FUT CC and FUT scenarios, respectively. THP related to recovery of the minimum ecological flows at S. Giustina and Mollaro reservoirs under FUT scenario is also presented.

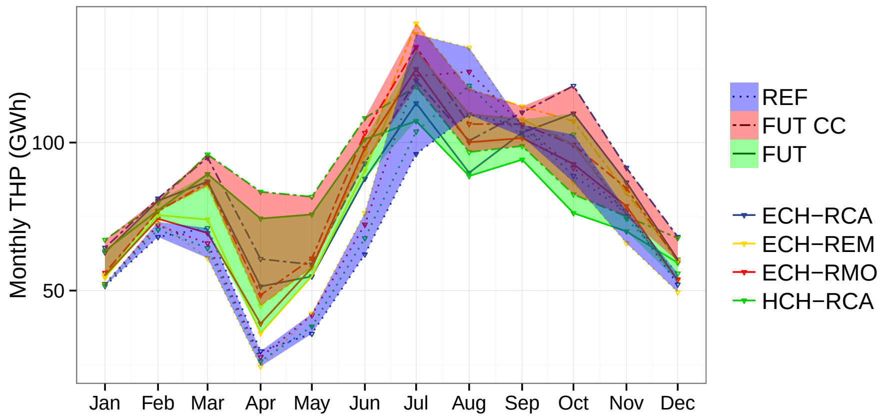


Figure 12: Monthly distribution of total Technical Hydropower Potential (THP) for Noce river basin under REF, FUT and FUT CC scenarios, respectively. Shaded area indicate the CMs envelope for the respective scenario.

should be considered with caution since water discharge entering the Careser reservoir has been computed under the assumption of constant areal extension of the glacier. Furthermore, very large differences among hydrological simulations reflect epistemic uncertainty stemming from the use of a number of CMs, which is particularly critical in the Alpine region. In this respect CMs not respecting the fundamental criteria described in Deidda et al. (2013) have been considered non behavioral and therefore removed to avoid the risk of artificially inflating uncertainty. From a a Bayesian point of view this may be assimilated to the choice of an informed prior distribution of possible models (Beven, 2002; Sadegh and Vrugt, 2014). Simulations under the FUT scenario (including $MEF$) differ from FUT CC (without $MEF$) with the projected percentage changes in the diverted flows (with respect to REF scenario) decreasing by 9-10% for all the reservoirs and CM simulations (see Table 7). In particular, for the reservoirs of Careser, Malga Mare and Pian Palù, 3 out of 4 CM simulations project a reduction in the diverted flow with respect to REF period as a consequence of the introduction of $MEF$.

The impact of climate change on technical hydropower potential is illustrated in Fig. 11 and Table 8 for all the 5 hydropower plants considered in the present study and the same climatic and operating scenarios considered previously, i.e. REF, FUT and FUT CC. Under the FUT CC scenario THP is projected to increase at Malga Mare and Cogolo 1 hydropower plants (see Fig. 1) as a consequence of the melting of the Careser and La Mare glaciers and of the projected increase of precipitation. Projected variations for the different CMs are in the range between 61% and 213% for Careser, and in the range between 47% and 106% for Malga Mare, respectively. Fig. 11 also shows that under FUT scenario projected variations are lower than in the FUT CC scenario but, however, higher than that under the REF scenario. As a consequence, for the powerplants in the headwaters the constraints introduced by $MEF$ releases do not fully counterbalance the increase of THP due to climate change only. Notice that for both FUT and FUT CC scenarios the largest projected variations for Careser are associated to ECH-RCA model as a consequence of the rather low temperatures projected under the REF scenario. In particular, mean monthly temperatures in the Careser area for ECH-RCA during REF resulted much lower than those obtained by the other CMs, and exceeded the value of zero only in July and August, thereby causing a significant snow accumulation and a strong reduction in the simulated streamflow feeding the reservoir.

Table 8: Average annual Technical Hydropower Potential (THP) for each of the 5 hydropower plants considered in the present study with reference to REF, FUT CC and FUT scenarios, respectively [a].

| **Model** | ECH-RCA | | | ECH-REM | | |
|---|---|---|---|---|---|---|
| **Period** | *REF [GWh]* | *FUT CC [GWh (%)]* | *FUT [GWh (%)]* | *REF [GWh]* | *FUT CC [GWh (%)]* | *FUT [GWh (%)]* |
| *Cogolo2* | 87.9 | 100.0 (13.8%) | 91.6 (4.3%) | 90.1 | 94.4 (4.8%) | 86.0 (-4.6%) |
| *Malga Mare* | 13.9 | 43.5 (213.4%) | 40.7 (193.5%) | 25.5 | 42.6 (66.9%) | 39.9 (56.1%) |
| *Cogolo1* | 70.4 | 145.2 (106.2%) | 134.8 (91.4%) | 97.7 | 146.7 (50.2%) | 136.6 (39.8%) |
| *Taio* | 385.4 | 446.9 (16.0%) | 396.8 + 21.5[b] (8.5%) | 398.5 | 435.5 (9.3%) | 386.4 + 21.6[b] (2.4%) |
| *Mezzocorona* | 289.2 | 327.6 (13.3%) | 296.9 + 5.8[b] (4.6%) | 292.4 | 318 (8.8%) | 286.6 + 5.8[b] (0.0%) |

| **Model** | ECH-RMO | | | HCH-RCA | | |
|---|---|---|---|---|---|---|
| **Period** | *REF [GWh]* | *FUT CC [GWh (%)]* | *FUT [GWh (%)]* | *REF [GWh]* | *FUT CC [GWh (%)]* | *FUT [GWh (%)]* |
| *Cogolo2* | 91.4 | 91.5 (0.2%) | 83.4 (-8.7%) | 90.7 | 88.4 (-2.6%) | 79.5 (-12.4%) |
| *Malga Mare* | 26.1 | 42.0 (60.8%) | 39.3 (50.4%) | 21.9 | 46.2 (111.5%) | 43.5 (98.9%) |
| *Cogolo1* | 100.1 | 146.9 (46.8%) | 136.7 (36.5%) | 90.3 | 178.6 (97.7%) | 168.8 (86.9%) |
| *Taio* | 396.1 | 426.7 (7.7%) | 376.8 + 21.2[b] (0.5%) | 385.9 | 425.5 (10.3%) | 374.4 + 20.9[b] (2.4%) |
| *Mezzocorona* | 292.6 | 312.9 (6.9%) | 282.4 + 5.8[b] (-1.5%) | 287.7 | 317.3 (10.3%) | 284.6 + 5.8[b] (0.9%) |

[a] Values within parentheses show the percentage anomalies of THP with respect to the associated CM REF simulation.
[b] Under FUT scenario THP related to the recovery of the minimum ecological flows at S. Giustina and Mollaro reservoirs is also presented.

For Cogolo 2 CM simulations differ significantly as a consequence of the conflicting projected variations in precipitation in the South-western part of the catchment. Fig. 11 and Table 8 indicate, under FUT CC scenario, a THP increase in 3 out of 4 climate simulations with projected changes in the range between -3% and 14%. The introduction of $MEF$ counterbalances the increase of THP due to climate change leading in three out of four cases to a reduction of THP with respect to the REF scenario.

At Taio and Mezzocorona hydropower plants, which are both located at low to intermediate altitudes, simulations conducted under FUT CC scenario show similar results (see Fig. 11). Projected THP increases are in the range between 8% and 16% for S. Giustina, and between 7% and 13% for Mollaro, respectively. Notice that $MEF$ is set to zero in these simulations such as the production of the ancillary small power plans at the toe of the S. Giustina and Mollaro reservoirs, which have been build specifically to recover part of the production lost in the main power plants because of the release. On the contrary, $MEF$ releases downstream the reservoirs are accounted for in the evaluation of hydropower potential under FUT scenario. In particular, monthly variability of $MEF$ releases for the time period 2040-2070 have been implemented following the prescriptions of the PGUAP (2006). Table 8 shows for the two reservoirs the separate contribution of the THP associated to the $MEF$ recovery and production at the associated power plant under the FUT scenario, as well as the percentage variations of the total THP with respect to the REF scenario. Inspection of Fig. 11 also suggests some considerations: i) despite the maximum flows associated to the $MEF$ recovery plants are similar (i.e. 3.68 and 3.79 $m^3/s$, see Table 2), THP differs significatively between the reservoirs ($\sim$ 21 GWh and $\sim$ 6 GWh, for S. Giustina and Mollaro, respectively) as a consequence of the large difference in the available gross hydraulic head $H$ (see Table 1); ii) projections at the two reservoirs indicate that the total THP reduces with respect to FUT CC scenario when $MEF$ is introduced, with the overall effect being larger at Mollaro than at S. Giustina; iii) simulations at Mollaro indicate that THP under FUT scenario will be close to that obtained under REF scenario (variations in the range between -2% and 5%) thus supporting the evidence that in the lower part of the catchment $MEF$ releases, even if partially recovered for hydropower production, will likely cancel additional revenues associated to the projected increases of inflows as foreseen by simulations driven only by climate change modifications.

Table 9: Total monthly Technical Hydropower Potential (THP) for the Noce river basin. CM averages for FUT CC and FUT scenarios are expressed in terms of percentage anomalies with respect to the associated CM REF simulation.

| **Model** | ECH-RCA | | | ECH-REM | | | ECH-RMO | | | HCH-RCA | | |
|---|---|---|---|---|---|---|---|---|---|---|---|---|
| **Period** | *REF [GWh]* | *FUT CC [%]* | *FUT [%]* | *REF [GWh]* | *FUT CC [%]* | *FUT [%]* | *REF [GWh]* | *FUT CC [%]* | *FUT [%]* | *REF [GWh]* | *FUT CC [%]* | *FUT [%]* |
| *Winter* | 190.8 | 26.0 | 20.6 | 186.2 | 16.9 | 9.5 | 190.3 | 15.3 | 4.6 | 187.0 | 29.9 | 22.9 |
| *Spring* | 127.2 | 67.0 | 52.5 | 142.8 | 39.2 | 26.8 | 141.5 | 50.2 | 37.6 | 131.7 | 107.5 | 90.7 |
| *Summer* | 311.3 | 6.6 | -1.5 | 373.3 | -0.7 | -6.7 | 352.4 | -2.2 | -7.4 | 325.0 | -3.2 | -10.7 |
| *Autumn* | 217.4 | 28.3 | 18.2 | 202.2 | 23.9 | 13.3 | 222.4 | 9.7 | 1.1 | 232.8 | -3.3 | -11.7 |
| *Total* | 846.7 | 25.6 | 16.6 | 904.5 | 14.7 | 6.4 | 906.5 | 12.6 | 4.2 | 876.5 | 20.5 | 11.4 |

The likely impacts of the selected scenarios on monthly THP for the entire Noce river basin are illustrated in Fig. 12. On annual basis simulations suggest a total THP increase for both FUT CC (in the range between 13% and 26%) and FUT (in the range between 4% and 17%) scenarios with respect to REF. On average it is likely that minimum flow requirements reduce hydropower potential by $\sim 8-9\%$ with respect to the case in which only the increase due to climate change is considered (see Table 9). For both FUT CC and FUT scenarios THP increases in winter, spring and autumn, while it decreases in summer, particularly in August. The only exception is represented by simulations conducted with HCH-RCA model which projects THP to decrease also in autumn ($-3\%$ and $-11\%$ for FUT CC and FUT scenarios, respectively) as a consequence of the projected decrease of precipitation (see Table 5). Fig. 12 also shows that the differences between FUT and FUT CC scenarios are almost homogeneous throughout the year with slightly higher deviations during spring, which is the season presenting the highest values of $MEF$ (PGUAP, 2006). This simulated change in monthly hydropower potential for the Noce river basin with respect to REF scenario (which is strictly connected to a shift in water availability) is likely to be observed throughout the Alps (see e.g., Finger et al., 2012; Hänggi and Weingartner, 2012; Gaudard et al., 2014; Maran et al., 2014). In particular, the reduction of snowfall accumulation due to the increase of temperature will likely limit the transfer of streamflow volumes from winter to late spring and summer and thus will suggest hydropower companies to change water management strategies if they want to maximize the revenue.

## 8. Conclusions

In the present work, future scenarios of water resources and hydropower potential production of the Noce catchment have been developed by using as climatic forcing the projections on an ensemble of 4 climatic models. The catchment is located in Southestern Alps and with its size of $1,367\ km^2$ represents the typical scale at which decisions about water resources management are taken. A challenging aspect of these simulations is the large uncertainty related to the spatial distribution of precipitation, which the climate models are not able to reproduce with the needed accuracy. It is acknowledged that the analysis of uncertainty is limited only to that arising from climate model selections.

Nevertheless, the study provides to date the most robust estimate of future changes for water resources availability in the region..

Hydrological simulations were conducted with GEOTRANSF, a geomorphically based hydrological model, after careful calibration against observed streamflow in the period 2000-2006. The whole modeling chain, from bias correction, downscaling of the precipitations and hydrological modeling, was validated against the relevant statistics of streamflow in the period 1970-2000, which was assumed as reference period. Resorting to bias correction was needed in order to properly account for local climatology and orographic effects which were not correctly reproduced by the outputs of available climate models.

Projections provided by the selected ensemble of 4 climate models runs for the period 2040-2070 showed an increase of the mean temperature in the range 2 - 4 K, whilst precipitation is much more uncertain with an increase of annual mean in the range between 2% and 6%. However, the increase of precipitation was not uniform, since larger increases accompanied by larger inter-model differences are observed at higher elevations. As a consequence, hydrological simulations show an increase of water yield during the period 2040-2070 with respect to 1970-2000, accompanied by an early spring melting, which leads to a shift from glacio-nival to nival regime for the catchment.

Magnitude of changes in both runoff and hydropower potential are location-dependent and in general larger at higher elevations as a consequence of the spatially non uniform increase of precipitation. The relative increase of the incoming streamflow is indeed larger for reservoirs at the higher elevations, i.e. Careser and Malga Mare, which respect those at the lower altitudes (S. Giustina and Mollaro). These simulations provide a baseline against which hydropower companies may confront their management strategies, possibly modifying them to take into account the effect of climate change in addition to the variability of the energy market. This is in line with recent findings in Swiss and Western-Italian Alps (Hänggi and Weingartner, 2012; Gaudard et al., 2014).

Finally, two different future scenarios, with and without the inclusion of the required minimum ecological flow recently implemented in the regional water resources policy, were compared in term of their impact on hydropower potential. Simulations indicate that in the lower part of the catchment releases from the reservoirs imposed by the recent regulations causes a reduction of the hydropower potential that almost cancel the gain associated to the projected increase of streamflow due to climate change.

## Acknowledgments

This research has been partially funded by European Union FP7 Collaborative Research Project CLIMB (Climate Induced Changes on the Hydrology of Mediterranean Basins, Grant 244151) and by the Italian Ministry of Public Instruction, University and Research through the project PRIN 2010-2011 (Innovative methods for water resources management under hydro-climatic uncertainty scenarios, prot. 2010JHF437). Authors also thank Autonomous Province of Trento for data provision.

## References

Badas, M. G., Deidda, R., Piga, E., 2006. Modulation of homogeneous space-time rainfall cascades to account for orographic influences. Nat. Hazards Earth Sys. Sci. 6, 427–437.

Barnes, S. L., 1964. A technique for maximazing details in numerical weather map analysis. J. Appl. Meteor. 3, 396–409.

Barnes, S. L., 1973. Mesoscale objective analysis using weighted timesetime observations. NOAA Tech. Memo. ERL NSSL-62. Tech. rep., National Severe Storms Laboratory, Norman, OK.

Bavay, M., Gränewald, T., Lehning, M., 2013. Response of snow cover and runoff to climate change in high Alpine catchments of Eastern Switzerland. Advances in Water Resources 55, 4 – 16.

Bellin, A., Majone, B., Cainelli, O., Alberici, D., VIlla, F., 2015. GEOTRANSF: A continuous coupled hydrological and water resources management model. Env. Model. Soft., (under review).

Beniston, M., 2006. Mountain Weather and Climate: A General Overview and a Focus on Climatic Change in the Alps. Hydrobiologia 562 (1), 3–16.

Beniston, M., 2012a. Impacts of climatic change on water and associated economic activities in the Swiss Alps. Journal of Hydrology 412-413, 291–296.

Beniston, M., 2012b. Is snow in the Alps receding or disappearing? Wiley Interdisciplinary Reviews: Climate Change 3 (4), 349–358.

Beniston, M., Stoffel, M., 2014. Assessing the impacts of climatic change on mountain water resources. Science of The Total Environment 493 (0), 1129 – 1137.
URL http://www.sciencedirect.com/science/article/pii/S0048969713014265

Beniston, M., Stoffel, M., Hill, M., 2011. Impacts of climatic change on water and natural hazards in the Alps: Can current water governance cope with future challenges? Examples from the European "ACQWA" project. Environmental Science and Policy 14 (7), 734–743.

Berg, P., Feldmann, H., Panitz, H.-J., 2012. Bias correction of high resolution regional climate model data. Journal of Hydrology 448-449, 80 – 92. URL http://www.sciencedirect.com/science/article/pii/S0022169412003010

Beven, K., 2002. Towards a coherent philosophy for modelling the environment. Proceedings of the Royal Society A: Mathematical, Physical and Engineering Sciences 458 (2026), 2465–2484.

Brugnara, Y., Brunetti, M., Maugeri, M., Nanni, T., Simolo, C., 2012. High-resolution analysis of daily precipitation trends in the central alps over the last century. International Journal of Climatology 32 (9), 1406–1422. URL http://dx.doi.org/10.1002/joc.2363

Brunetti, M., Lentini, G., Maugeri, M., Nanni, T., Auer, I., Böhm, R., Schöner, W., 2009. Climate variability and change in the Greater Alpine Region over the last two centuries based on multi-variable analysis. International Journal of Climatology 29 (15), 2197–2225. URL http://dx.doi.org/10.1002/joc.1857

Brunetti, M., Maugeri, M., Nanni, T., Auer, I., Böhm, R., Schöner, W., 2006. Precipitation variability and changes in the greater Alpine region over the 1800-2003 period. Journal of Geophysical Research: Atmospheres 111 (D11). URL http://dx.doi.org/10.1029/2005JD006674

Caldeira, K., Jain, A., Hoffert, M., 2003. Climate sensitivity uncertainty and the need for energy without co2 emission. Science 299 (5615), 2052–2054.

Cane, D., Barbarino, S., Renier, L., Ronchi, C., 2013. Regional climate models downscaling in the Alpine area with multimodel superensemble. Hydrology and Earth System Sciences 17 (5), 2017–2028.

Carturan, L., Baroni, C., Becker, M., Bellin, A., Cainelli, O., Carton, A., Casarotto, C., Dalla Fontana, G., Godio, A., Martinelli, T., Salvatore, M., Seppi, R., 2013. Decay of a long-term monitored glacier: Careser Glacier (Ortles-Cevedale, European Alps). Cryosphere 7 (6), 1819–1838.

Castagna, M., Bellin, A., 2009. A bayesian approach for inversion of hydraulic tomographic data. Water Resour. Res. 45.

Chen, J., Brissette, F., Poulin, A., Leconte, R., 2011. Overall uncertainty study of the hydrological impacts of climate change for a canadian watershed. Water Resources Research 47 (12).

Chiogna, G., Santoni, E., Camin, F., Tonon, A., Majonea, B., Trenti, A., Bellin, A., 2014. Stable Isotope Characterization of the Vermigliana Catchment. Journal of Hydrology 509, 295–305.

Deidda, R., 2000. Rainfall downscaling in a space-time multifractal framework. Water Resour. Res. 36, 1779–1794.

Deidda, R., Badas, M. G., Piga, E., 2004. Space-time scaling in high-intensity Tropical Ocean Global Atmosphere Coupled Ocean-Atmosphere Response Experiment (TOGA-COARE) storms. Water Resour. Res. 40, W02506.

Deidda, R., Badas, M. G., Piga, E., 2006. Space-time Multifractality of Remotely Sensed Rainfall Fields. Journal of Hydrology 322, 2–13.

Deidda, R., Marrocu, M., Caroletti, G., Pusceddu, G., Langousis, A., Lucarini, V., Puliga, M., Speranza, A., 2013. Regional climate models' performance in representing precipitation and temperature over selected Mediterranean areas. Hydrology and Earth System Sciences 17 (12), 5041–5059. URL http://www.hydrol-earth-syst-sci.net/17/5041/2013/

European Commission, 2000. Directive 2000/60/EC of the European Parliament and of the Council of 23 October 2000 Establishing a Framework for Community Action in the Field of Water Policy.

Farinotti, D., Usselmann, S., Huss, M., Bauder, A., Funk, M., 2012. Runoff evolution in the Swiss Alps: projections for selected high-alpine catchments based on ENSEMBLES scenarios. Hydrological Processes 26 (13), 1909–1924.

Finger, D., Heinrich, G., Gobiet, A., Bauder, A., 2012. Projections of future water resources and their uncertainty in a glacierized catchment in the Swiss Alps and the subsequent effects on hydropower production during the 21st century. Water Resources Research 48 (2).

François, B., Hingray, B., Hendrickx, F., Creutin, J., 2014. Seasonal patterns of water storage as signatures of the climatological equilibrium between resource and demand. Hydrology and Earth System Sciences 18 (9), 3787–3800.

Funtowicz, S. O., Ravetz, J. R., 1990. Uncertainty and Quality in Science for Policy. Kluwer Academic Publishers, Dordrecht, The Netherlands.

Gaudard, L., Gilli, M., Romerio, F., 2013. Climate Change Impacts on Hydropower Management. Water Resources Management 27 (15), 5143–5156.

Gaudard, L., Romerio, F., 2014. The future of hydropower in Europe: Interconnecting climate, markets and policies. Environmental Science and Policy 37, 172–181.

Gaudard, L., Romerio, F., Dalla Valle, F., Gorret, R., Maran, S., Ravazzani, G., Stoffel, M., Volonterio, M., 2014. Climate change impacts on hydropower in the Swiss and Italian Alps. Science of the Total Environment 493, 1211–1221.

Gelman, A., Carlin, J. B., Stern, H. S., Rubin, D. B., 1995. Bayesian Data Analysis. Chapman & Hall.

Gill, M. K., Kaheil, Y. H., Khalil, A., McKee, M., Bastidas, L., 2006. Multiobjective particle swarm optimization for parameter estimation in hydrology. Water Resources Research 42 (7).

Gobiet, A., Kotlarski, S., Beniston, M., Heinrich, G., Rajczak, J., Stoffel, M., 2014. 21st century climate change in the European Alps: A review. Science of The Total Environment 493 (0), 1138 – 1151. URL http://www.sciencedirect.com/science/article/pii/S0048969713008188

Graveline, N., Majone, B., Duiden, R. V., Ansink, E., 2014. Hydro-economic modeling of water scarcity under global change: an application to the Gállego river basin (Spain). Reg. Environ. Change 14 (1), 119–132.

GSE, 2013. Statistical report 2012 - renewable energy power plants - electric sector. Tech. rep., Gestore Servizi Energetici, available at http://www.gse.it/it/Statistiche/RapportiStatistici/Pagine/default.aspx.

Hamududu, B., Killingtveit, A., 2012. Assessing climate change impacts on global hydropower. Energies 5 (2), 305–322.

Hänggi, P., Weingartner, R., 2012. Variations in Discharge Volumes for Hydropower Generation in Switzerland. Water Resources Management 26 (5), 1231–1252.

Hawkins, E., Sutton, R., 2009. The potential to narrow uncertainty in regional climate predictions. Bulletin of the American Meteorological Society 90 (8), 1095–1107.

Haylock, M. R., Hofstra, N., Klein-Tank, A. M. G., Klok, E. J., Jones, P. D., New, M., 2008. A European daily high-resolution gridded data set of

surface temperature and precipitation for 1950-2006. J. Geophys. Res. 113, D20119.
Heikkinen, R., Luoto, M., Araújo, M., Virkkala, R., Thuiller, W., Sykes, M., 2006. Methods and uncertainties in bioclimatic envelope modelling under climate change. Progress in Physical Geography 30 (6), 751–777.
IPCC SRES, 2000. Special Report on Emissions Scenarios: A special report of Working Group III of the Intergovernmental Panel on Climate Change. Cambridge University Press.
Jasper, K., Calanca, P., Gyalistras, D., Fuhrer, J., 2004. Differential impacts of climate change on the hydrology of two alpine river basins. Climate Research 26 (2), 113–129.
Kay, A., Davies, H., Bell, V., Jones, R., 2009. Comparison of uncertainty sources for climate change impacts: Flood frequency in england. Climatic Change 92 (1-2), 41–63.
Kennedy, J., Eberhart, R., 1995. Particle swarm optimization. In: Proceedings of IEEE International Conference on Neural Networks. pp. 1942–1948.
Kirchner, J. W., 2009. Catchment as simple dynamical systems: Catchment characterization, rainfall-runoff modeling, and doing hydrology backward. Journal of Hydrology 45, W02429.
Koch, F., Prasch, M., Bach, H., Mauser, W., Appel, F., Weber, M., 2011. How Will Hydroelectric Power Generation Develop under Climate Change Scenarios? A Case Study in the Upper Danube Basin. Energies 4 (10), 1508–1541.
Kowalsky, M., Finsterle, S., Rubin, Y., JUN 2004. Estimating flow parameter distributions using ground-penetrating radar and hydrological measurements during transient flow in the vadose zone. Advances in Water Resources 27 (6), 583–599.
Kumar, A., Schei, T., Ahenkorah, A., Rodriguez, R., Devernay, J., Freitas, M., Hall, D., Killingtveit, Å., Liu, Z., 2011. Hydropower. In: Edenhofer, O., Pichs-Madruga, R., Sokona, Y., Seyboth, K., Matschoss, P., Kadner, S., Zwickel, T., Eickemeier, P., Hansen, G., Schlömer, S., von Stechow, C. (Eds.), IPCC Special Report on Renewable Energy Sources and Climate Change Mitigation. Cambridge University Press, Cambridge, United Kingdom and New York, NY, USA.
Kundzewicz, Z., Kanae, S., Seneviratne, S., Handmer, J., Nicholls, N., Peduzzi, P., Mechler, R., Bouwer, L., Arnell, N., Mach, K., Muir-Wood, R., Brakenridge, G., Kron, W., Benito, G., Honda, Y., Takahashi, K., Sherstyukov, B., 2014. Flood risk and climate change: global and regional perspectives [le risque d'inondation et les perspectives de changement climatique mondial et regional]. Hydrological Sciences Journal 59 (1), 1–28.
La Jeunesse, I., Cirelli, C., Aubin, D., Larrue, C., Sellami, H., Bellin, A., Benabdallah, S., Bird, D., Deidda, R., Dettori, M., Engin, G., Herrmann, F., Ludwig, R., Mabrouk, B., Majone, B., Paniconi, C., Soddu, A., 2015. Is climate change a threat for water uses in the Mediterranean region? Results from a survey at local scale. Science of The Total Environment, (submitted).
Laghari, A. N., Vanham, D., Rauch, W., 2012. To what extent does climate change result in a shift in Alpine hydrology? A case study in the Austrian Alps. Hydrological Sciences Journal 57 (1), 103–117.
Lambrecht, A., Mayer, C., 2009. Temporal variability of the non-steady contribution from glaciers to water discharge in western austria. Journal of Hydrology 376 (3-4), 353–361.
Liston, G. E., Elder, K., 2006. A Meteorological Distribution System for High-Resolution Terrestrial ModModel (MicroMet). J. Hydrometeo. 7, 217–234.
Ludwig, R., Soddu, A., Duttmann, R., Baghdadi, N., S., B., Deidda, R., Marrocu, M., Strunz, G., Wendland, F., Engin, G., Paniconi, C., Prettenthaler, F., Lajeunesse, I., Afifi, S., Cassiani, G., Bellin, A., Mabrouk, B., Bach, H., Ammerl, T., 2010. Climate-induced changes on the hydrology of mediterranean basins - A research concept to reduce uncertainty and quantify risk. Fresen. Environ. Bull. 19(10 A), 2379–2384.
Majone, B., Bertagnoli, A., Bellin, A., 2010. A non-linear runoff generation model in small Alpine catchments. Journal of Hydrology 385 (1-4), 300–312.
Majone, B., Bovolo, C. I., Bellin, A., Blenkinsop, S., Fowler, H. J., 2012. Modeling the impacts of future climate change on water resources for the Gàllego river basin (Spain). Water Resources Research 48, W01512.
Maran, S., Volonterio, M., Gaudard, L., 2014. Climate change impacts on hydropower in an alpine catchment. Environmental Science and Policy 43, 15–25.
Markoff, M., Cullen, A., 2008. Impact of climate change on pacific northwest hydropower. Climatic Change 87 (3-4), 451–469.
Meteotrentino, 2011. Evoluzione e monitoraggi recenti dei ghiacciai trentini. Trento.
URL `http://www.meteotrentino.it`
Minville, M., Brissette, F., Krau, S., Leconte, R., 2009. Adaptation to climate change in the management of a canadian water-resources system exploited for hydropower. Water Resources Management 23 (14), 2965–2986.
Morgan, M., Mellon, C., 2011. Certainty, uncertainty, and climate change. Climatic Change 108 (4), 707–721.
Murphy, J., Sexton, D., Barnett, D., Jones, G., Webb, M., Collins, M., Stainforth, D., 2004. Quantification of modelling uncertainties in a large ensemble of climate change simulations. Nature 430 (7001), 768–772.
PGUAP, 2006. Piano Generale di Utilizzazione delle Acque Pubbliche. Trento.
URL `http://pguap.provincia.tn.it/`
Raje, D., Mujumdar, P., 2010. Reservoir performance under uncertainty in hydrologic impacts of climate change. Advances in Water Resources 33 (3), 312–326.
Rixen, C., Teich, M., Lardelli, C., Gallati, D., Pohl, M., Ptz, M., Bebi, P., 2011. Winter tourism and climate change in the Alps: An assessment of resource consumption, snow reliability, and future snowmaking potential. Mountain Research and Development 31 (3), 229–236.
Sadegh, M., Vrugt, J., 2014. Approximate bayesian computation using markov chain monte carlo simulation: Dream(abc). Water Resources Research 50, Article in Press.
Schaefli, B., Hingray, B., Musy, A., 2007. Climate change and hydropower production in the Swiss Alps: Quantification of potential impacts and related modelling uncertainties. Hydrology and Earth System Sciences 11 (3), 1191–1205.
Tebaldi, C., Knutti, R., 2007. The use of the multi-model ensemble in probabilistic climate projections. Philosophical Transactions of the Royal Society A: Mathematical, Physical and Engineering Sciences 365 (1857), 2053–2075.
Tebaldi, C., Smith, R., Nychka, D., Mearns, L., 2005. Quantifying uncertainty in projections of regional climate change: A bayesian approach to the analysis of multimodel ensembles. Journal of Climate 18 (10), 1524–1540.

Teutschbein, C., Seibert, J., 2012. Bias correction of regional climate model simulations for hydrological climate-change impact studies: Review and evaluation of different methods. Journal of Hydrology 456–457, 12 – 29.

Vicuna, S., Dracup, J., Lund, J., Dale, L., Maurer, E., 2010. Basin-scale water system operations with uncertain future climate conditions: Methodology and case studies. Water Resources Research 46 (4).

Vicuna, S., Leonardson, R., Hanemann, M., Dale, L., Dracup, J., 2008. Climate change impacts on high elevation hydropower generation in california's sierra nevada: A case study in the upper american river. Climatic Change 87 (1 SUPPL), S123–S137.

Viviroli, D., Archer, D., Buytaert, W., Fowler, H., Greenwood, G., Hamlet, A., Huang, Y., Koboltschnig, G., Litaor, M., Lopez-Moreno, J., Lorentz, S., Schädler, B., Schreier, H., Schwaiger, K., Vuille, M., Woods, R., 2011. Climate change and mountain water resources: Overview and recommendations for research, management and policy. Hydrology and Earth System Sciences 15 (2), 471–504.

Viviroli, D., Weingartner, R., 2004. The hydrological significance of mountains: from regional to global scale. Hydrology and Earth System Sciences 8 (6), 1016–1029.

Wilby, R., Dessai, S., 2010. Robust adaptation to climate change. Weather 65 (7), 180–185.

Wilby, R., Harris, I., 2006. A framework for assessing uncertainties in climate change impacts: Low-flow scenarios for the river thames, uk. Water Resources Research 42 (2).

Yilmaz, K., Gupta, H., Wagener, T., 2008. A process-based diagnostic approach to model evaluation: Application to the NWS distributed hydrologic model. Water Resources Research 44 (9).

Zimmermann, M., 2001. Energy situation and policy in Switzerland. International Journal of Ambient Energy 22 (1), 29–34.